Method Development of Multi-Layered Optical Skin Phantoms

Master's thesis in Biotechnology

LOUISE ECKERSTRÖM

DEPARTMENT OF PHYSICS

CHALMERS UNIVERSITY OF TECHNOLOGY
Gothenburg, Sweden 2025
www.chalmers.se

Master's thesis 2025

Method Development of Multi-Layered Optical Skin Phantoms

LOUISE ECKERSTRÖM

CHALMERS
UNIVERSITY OF TECHNOLOGY

Department of Physics
Chalmers University of Technology
Gothenburg, Sweden 2025

Method Development of Multi-Layered Optical Skin Phantoms
LOUISE ECKERSTRÖM

Supervisors: Marcus Andersson and Sofia Dall'Orso, Odinwell
Examiner: Julie Gold, Department of Physics

Master's Thesis 2025
Department of Physics
Chalmers University of Technology
SE-412 96 Gothenburg
Telephone +46 31 772 1000

Typeset in LaTeX
Printed by Chalmers Reproservice
Gothenburg, Sweden 2025

Method Development of Multi-Layered Optical Skin Phantoms
LOUISE ECKERSTRÖM
Department of Physics
Chalmers University of Technology

Abstract

The increasing research interest in and use of optical medical technologies has led to a growing need for synthetic testing materials with tissue-mimicking optical properties, known as optical phantoms. Many different materials and methods have been used to create such phantoms but the field currently lacks standardization and repeated results. Optical phantoms made for dark skin tones and for short wavelengths of light are also missing from research.

This project tests and builds on previously established methods for creating optical phantoms made out of PDMS silicone. A method for creating a multi-layered skin phantom in which each layer mimics the thickness and absorption of one of the main layers of human skin is developed and presented. Four versions of this phantom are made: two of them mimic the absorption of fair skin and two of them the absorption of dark skin. For each skin colour, one of the phantoms mimic the absorption at a wavelength of 405 nm and the other the absorption at 630 nm.

A correlation between the concentration of nigrosin (an absorbing agent) and the absorption coefficient of the resulting phantoms is determined using spectrometry. This correlation can work as a guide for how to reach a desired absorption coefficient.

Keywords: optical phantom, skin, multi-layered, absorption.

Acknowledgements

I would like to thank Marcus Andersson for letting me take on this project and introducing me to the company, and to everyone at Odinwell for a very warm welcome, some really fun quiz fikas, and nice chats on the sunny parking lot. A special thank you to my supervisor Sofia Dall'Orso for your guidance in the lab and for answering my many (many!) questions. Working alongside you all has been truly great. Also thanks to Julie Gold for agreeing to take on this project as an examiner and using your contacts in the research world to try to find me an integrating sphere to use. Lastly, thank you to my family and friends for always cheering me on!

Louise Eckerström, Gothenburg, June 2025

Contents

1
Project specification

This chapter describes the overarching parameters and goals of the entire project. It is followed by a literature study to figure out the best options for reaching the goals while staying within the practical limitations. The rest of the report will then focus on the specific alternative that is decided on in the literature study.

This master's thesis has been done in cooperation with and at the request of the company Odinwell, a Swedish start-up company in the field of optical medical technologies. Odinwell is currently developing an optical biosensor that can be added into wound dressings to closely monitor wounds in real time. The biosensor uses fiber optics to detect biomarkers for bacterial growth, like porphyrin, as well as for blood and other fluids [1].

In order to fine-tune and calibrate the biosensor, the biosensor has to be tested on materials that are relevant to the intended usage of the instrument. The golden standard is of course to test the instrument in a real scenario, in this case on the wound and skin of a living human, but that is oftentimes impractical, expensive, and ethically dubious, especially during the development phase. Alternative test systems are therefore typically used during product development. So far, Odinwell has mostly used very simple test systems with few similarities to the intended usage, like ethanol-dissolved porphyrin on white paper, to test their sensor, but the mission of this thesis is to develop a more complex, tunable, and life-like test system to aid in the development of the sensor.

More specifically, there were a number of requirements, wants, and limitations from Odinwell on the test system that would be developed in this project. The test system should:

- be a relevant substitute for healthy, living human skin.
- mimic the relevant optical properties of real skin, specifically for the wavelengths 405 nm and 630 nm.
- be stable over time.
- be homogeneous.
- be cheap and easy to make with the available lab equipment.

- ideally, work as a stable porphyrin model through the incorporation of PpIX during the production.

Odinwell's biosensor is, as mentioned above, meant to be used on wounds, but there are several reasons why a model of healthy skin is of interest anyway. Firstly, sensors will probably be placed both on the wound itself and on the surrounding skin, to get a healthy reference for the individual patient and to estimate the area of the wound. Secondly, wounds will develop and be covered by skin as they heal, so their optical properties will approach those of healthy skin during healing. This could work as another marker for healing.

The model should mimic the optical properties of skin but does not need to mimic any other property of real tissue, as the sensor only uses optical measurement methods. The sensor uses light with a wavelength of 405 nm to excite porphyrin and make it fluoresce, which is why the optical properties of skin at that specific wavelength should be mimicked. Light with the wavelength 630 nm is also commonly used in similar optical sensors, so a model should also be developed to match those optical properties.

Furthermore, the requirements of homogeneity, stability, and inexpensiveness are all due to similar reasons. A model has to have known and consistently reliable properties, preferably independent of time and the exact spot on the model, to be effective for calibrating a sensor on. The model should also be stable and cheap since a lot of repeated testing will have to be done on it during the early development stages of the sensor.

One major requirement of the project was that the model should be developed, verified, and created using the limited laboratory equipment available at Odinwell's facilities. The specifics of this will be discussed later in the report.

The goal of incorporating porphyrin into the model is set mostly to investigate whether this would be possible for future wound models made using the same techniques and materials, as porphyrin is not present in any large amounts on healthy skin, which this model is supposed to mimic.

In summary, this project will be specified and determined to a large extent by me, the thesis student, but with the goals and limitations set by Odinwell. Determining which option for creating this test model is the most suitable is an important part of the project itself.

2
Literature study

In this section, a few different options will be evaluated based on the test system criteria outlined in the project specification. The options that will be discussed are *in vivo* skin, *in vitro* skin, *ex vivo* skin, and optical phantoms. A decision of which option to continue with will be made at the end of the literature study.

2.1 *In vivo* skin

Before even looking into models that could work as a substitute for the situation or material you want to test on, the first question should be if a model is even needed, or if the testing can be done on the real situation of interest. In this case, this would mean testing the optical sensor on the skin of healthy human test subjects. This option is obviously ideal for accuracy and relevance, but it does bring some other challenges.

Before those challenges are discussed, it should be mentioned that the only reason that this is even an option in this early stage of development is because Odinwell's optical sensor is entirely safe and non-invasive, since it at this stage would only expose the skin of the test subjects to violet light (405 nm). Light of this wavelength is safe for human skin, assuming moderate exposure time and intensity [2]. The only health risk of this would be if the 405 nm light was shined directly into the subjects' eyes [3], but this can easily be avoided using basic caution and, for extra safety, orange-tinted safety goggles.

There are two alternatives for test subjects in this scenario: either using ourselves as test subjects or recruiting test subjects formally. If test subjects were formally recruited for a clinical trial, an ethical approval by the Swedish Ethical Review Authority (Etikprövningsmyndigheten) would be required [4]. This process can be expensive and complicated, and the company would have to rigoriously prove both the safety and the necessity of these tests. This alternative would also not be suitable for the simple and repeated testing and calibrating of the sensor during its early development phase. The other alternative, testing on our own skin, is therefore a more accessible, cheap, and reasonable option. Simple and informal testing of an obviously safe product on the researchers themselves is common during product development, but it is not an option for producing clinical data. For a clinical trial, an ethical approval is always needed [4].

In whatever way the test subjects would be chosen, the accuracy and relevance of the tests would be limited to the specific subjects we had access to. The optical properties of a test subject's skin are of course specific to that individual and not tunable for this testing. This would be especially problematic and skew the data if the test subjects all or mostly had similar skin colours, as the skin colour significantly affects the optical properties and penetration depth of light in skin [5]. Lack of testing on darker-skinned subjects has already introduced significant racial bias into optical medical technologies, making the available optical medical technologies today less sensitive and less accurate for dark-skinned patients [6].

One desired property of the testing system is homogeneity, since repeatable and reliable measurements are important when calibrating the sensor. Real *in vivo* skin is however not homogeneous but also includes for example hair, freckles, scars, and blood vessels, which might affect the local optical properties of the skin. The optical properties of *in vivo* skin are also not stable over time, as they may be affected by for example tanning or hydration [7].

Lastly, it would obviously not be ethical to incorporate porphyrin into the testing system if *in vivo* skin was used.

2.2 *In vitro* skin

In vitro skin samples, here defined as non-viable human skin donated from cadavers or from surgeries, is an obvious alternative for an optical skin model. The most common source of these skin samples is surgical waste from reductive surgeries [8], which makes this an option without serious ethical considerations. It does however mean that an ethics approval from the Swedish Ethical Review Authority would be required to use donated skin in the developmental research [4]. If an approval was granted, there would still be requirements on the handling of the tissues and the personal data of the donors, as well as on the acquisition of consent from the donors [4]. This whole process means that getting access to the skin samples would not be especially cheap nor easy.

Regarding the accuracy and relevancy of using *in vitro* skin as an optical model for healthy, living skin, it is not a perfect substitute. A meta-study on the published values of measured absorption and reduced scattering coefficients of *in vivo* and *in vitro* skin showed that the absorption coefficients were on average 2.4 times larger for *in vitro* than *in vivo*, while the reduced scattering coefficients were 1.7 times larger for *in vitro* than for *in vivo* skin [9]. The variability within the data is also much larger for the *in vitro* than the *in vivo* samples [9], making the results less certain. The variability may be partly due to differences in the specific method of preserving and handling of the skin sample [9, 8, 10]. The optical properties of the *in vitro* samples might also be affected by whether they were taken from a live subject or post-mortem, as biopsies from live subjects are usually exsanguinated while post-mortem samples often have remnants of clotted blood [9]. The differences in the

average measurements may also be attributed to the presence of underlying fresh blood in *in vivo* skin, as hemoglobin is a highly absorptive chromophore in skin [9, 11].

The optical properties of *in vitro* skin is not tunable, but depends on several patient-specific factors [9]. This means that if the donors all have similar skin colours and tones, you will only be able to test the optical device on that specific skin colour.

Additionally, *in vitro* skin samples are not stable for especially long after thawing and the optical properties will vary both within and between samples, due to irregularities in the skin (like hair or freckles) and due to patient-specific factors like skin colour, age, and health conditions [8, 9]. This means that *in vitro* skin samples can not be depended on for repeated and consistent optical measurements.

2.3 *Ex vivo* skin

Ex vivo skin is, in this report, defined as human skin that has been donated and kept alive outside of the human body. The donated skin usually comes from surgical interventions as surgical waste [12], so even though an ethical approval from the Swedish Ethical Review Authority would be needed for using this type of model [4], the ethical considerations are relatively small, especially considering the model is kept alive and can be tested on repeatedly so the need for new samples is minimized. *Ex vivo* skin is usually maintained at 37°C in a cell culture incubator, with a high CO_2 concentration in the internal atmosphere and with some kind of media [12]. The media usually contains some animal-based serum, but serum-free options have also been used successfully [12]. Viability testing, i.e. checking that the cells are still alive, is also necessary before the model is used [13]. Several different viability tests that detect different biological processes might need to be performed to get an accurate picture of the cells' viability [13]. All of this means that keeping an *ex vivo* skin model alive and functional for testing requires time, labour, and the right equipment.

Ex vivo skin is of course derived from and has a lot of similarities to *in vivo* skin, making it a good model in regards to accuracy [13]. It has however been noted that *ex vivo* skin lightens in colour during the first day of cultivation and then keeps that paler colour during the rest of the cultivation [12], indicating that the absorption would be underestimated when using an *ex vivo* model.

Donated skin samples have substantial optical heterogeneity both between samples from different donors and at different spots on the same sample [12]. These variations are differences in colours, thickness, and vascularisation [12]. Point variations within the same sample also include things like sebaceous glands and hair follicles [13]. The issue of different thicknesses can however be handled by slicing the samples thinly before culturing them [13]. The other sources of optical heterogeneity are harder to address and would result in different measured optical values depending on the specific source sample and the specific spot of the model that was measured.

Lastly, *ex vivo* skin can function as a porphyrin model by letting porphyrin-producing bacteria colonise the skin [14]. The concentration of porphyrins would however not be stable using this method.

2.4 Optical phantoms

Phantoms are materials that mimic the properties of a biological tissue [15], in this case human skin. The focus for this project is on mimicking specifically the optical properties, meaning that the phantoms of interest are optical human skin phantoms.

Optical phantoms can be made out of a wide variety of materials but usually includes a matrix material, a scattering agent, and an absorbing agent [15, 16]. Varying the concentrations of the absorbing and scattering agents changes the absorption coefficient and the reduced scattering coefficient respectively, meaning that the phantoms are optically tunable and can achieve a range of different optical properties [16, 17, 18]. This means that optical phantoms are just as suitable for mimicking dark skin as fair skin [6]. The choice of materials should however be made with the target optical properties in mind, as not all phantom materials are suitable for all possible optical properties. For example, the scattering agent needs to have a much higher refraction index than the matrix material if the goal is to make a highly scattering phantom, as the scattering occurs due to differences in refractive index [19]. The absorbing agent should also be able to achieve the target absorption coefficient while using a practicable concentration. It should also be mentioned that in order to even have relevant and reliable target properties for optical phantoms to mimic, there is a need for the optical properties of human skin to be experimentally determined in previous studies. The combined body of research on the optical properties of human skin is however not especially congruent, as different studies come to different results, but also use different methods and study skin from different body parts [5]. This is especially true for research on dark skin, since only a small minority of the subjects in studies that optically measure skin are dark-skinned [5].

The stability of phantoms is highly dependent on the choice of materials. Synthetic matrix materials like silicone or resin can make semi-permanent optical phantoms, while organic matrix materials like gelatin or agar are only stable for a few days or weeks [15, 16]. The absorbing and scattering agents should also be chosen to match the matrix material for optimal stability, so a synthetic matrix material should be matched with stable, synthetic agents [15].

Optical skin phantoms can be made to mimic the natural irregularities in human skin, like blood vessels [17], but they can also be made homogeneous with the same thickness and optical properties in every spot [16]. Phantoms can also be cheap and easy to make, but this varies depending on the chosen materials and methods.

Lastly, it is possible to incorporate porphyrin into an optical phantom and make

it relatively stable as long as a biologically compatible, organic matrix material is used [15]. These organic types of phantoms are however not stable for more than a few days or weeks even if no porphyrin is added, and the more stable, synthetic phantoms are generally not seen as compatible with organic compounds [15].

2.5 Comparison of options

The different options for a skin model that have been discussed above are *in vivo* skin, *in vitro* skin, *ex vivo* skin, and optical phantoms. Using the criteria for the test system outlined in the project specification, they will now be compared to each other. Fig. 2.1 below gives a side-by-side overview of the pros and cons of the different options.

	In vivo	*In vitro*	*Ex vivo*	Phantoms
Accurate	✓	x	✓	✓
Stable	x	x	✓	✓
Homogeneous	x	x	x	✓
Cheap/easy	✓/x	x	x	✓
Porphyrin	x	?	✓	✓/x

Figure 2.1: A comparison of four different skin model options, based on the criteria outlined in the project specification. A "✓" means that the model can fulfill the criterion, while an "×" means that it cannot.

Three out of those options - *in vivo, in vitro*, and *ex vivo* skin - are based on using real skin from humans, which comes with similar challenges. Firstly, they are all heterogeneous due to inherent irregularities in skin. Secondly, they all require ethical approval and correct handling of things like the personal data of the donors/-subjects, which complicates the process. Thirdly, their optical properties are not tunable, but set by a number of patient-specific factors, like skin colour. This makes the models highly dependent on the specific groups of subjects and can introduce a racial bias into the test system and therefore the technology. None of these things are an issue for optical phantoms, which makes phantoms more suitable for this test system in terms of homogeneity, ease of use, and accuracy for a wide population.

Regarding accuracy on an individual basis instead of on a population level, the results are slighty different. *In vivo* skin is of course the only truly accurate option on an individual basis, as that is the exact situation that the other options are trying to mimic. The optical properties of *in vitro* skin can vary significantly from *in vivo* skin and will also vary depending on the exact sampling and handling of the donated skin. *Ex vivo* skin is reported to lighten in colour during the first day of cultivation but stays stable after that, so can be presumed to have similar but slightly lower absorption than *in vivo* skin. Phantoms can be made to mimic any optical properties and are therefore also accurate, as long as the target values are

based on good data from *in vivo* skin.

Only *ex vivo* skin and phantoms have stable optical properties over time. *Ex vivo* skin will, as mentioned above, lighten at first but then stabilize after one day of culturing. The stability of phantoms is highly dependent on the choice of materials, since agar- or gelatin-based phantoms are only stable for a few days whereas synthetic phantoms made out of for example silicone or resin are semi-permanent and can be used consistently for months or even years. The optical properties of *in vivo* skin, on the other hand, can vary for several reasons such as tanning, health status, and the level of hydration. *In vitro* skin might be the least stable, as skin samples generally can only be used for a short time after thawing. The stability also influences the cheapness and ease of use of the test system, even if the constant maintenance requirements of *ex vivo* skin makes keeping that system stable an expensive and involved process. *In vivo* skin could however be considered a cheap and easy test system, but only if we choose to only test on ourselves, informally, instead of enlisting subjects and generating clinical data.

Lastly, the test system options are compared based on their potential as stable porphyrin models. *In vivo* skin is not suitable for this purpose, mostly for ethical reasons. It is unclear if *in vitro* skin could be used as a porphyrin model, as no sources on this could be found. It is however possible for *ex vivo* skin and for some phantoms, but only if the phantom matrix material is organic instead of synthetic. Using a synthetic matrix material would compromise the overall stability of the phantom, so the phantom can not be both stable over time and work as a porphyrin model.

Considering all of these comparisons, as illustrated in fig. 2.1, I chose to continue working with optical phantoms.

3
Introduction

This chapter will introduce the project, as chosen at the end of the literature study, and explain its place in the research field of optical phantoms. The chapter begins with a section on background and theory that contextualises the project, both societally and scientifically, and highlights the research areas that remain understudied. The purpose and research questions guiding the thesis are explained before the chapter ends with a discussion on the scope and limitations.

3.1 Background & Theory

A phantom is any synthetic material that simulates human or animal tissue by mimicking the properties of the biological tissue of interest [15]. Phantoms have been created for a wide variety of tissues - like brain, skin, and breast - and for many different purposes [15, 16, 20]. The mechanical, electrical, thermal, and acoustic properties of tissue have all been mimicked in different phantoms [15, 17]. This thesis will however solely focus on optical phantoms, meaning phantoms that mimic the optical properties of real human tissue.

Phantoms are used instead of real tissue for ethical and practical reasons, as well as because they have the potential to be cheaper, more stable over time, and to have known and tunable properties [17, 19, 21]. They can be used for the purposes of testing new sensors, comparing the performance of different sensors, doing quality control, or reducing the signal-to-noise ratio of sensors [15]. Optical phantoms specifically are often used for refining and calibrating instruments of laser therapy [22], noninvasive diffuse near-infrared spectroscopy (NIRS) [20], optical coherence tomography (OCT) [23], near-infrared (NIR) spectroscopy [15], and other optical diagnostic methods, using the phantoms instead of biological samples [23]. Studying the available literature reveals that most optical phantoms are made to mimic the optical properties of tissue in NIR or IR light, but this project will focus on phantoms for the shorter wavelengths 405 nm and 630 nm. Since melanin is especially absorbing in the UV range and has an absorption peak at 335 nm [24], the optical properties of a 405 nm skin phantom have to be very different from the more common NIR or IR skin phantoms. The wavelength 405 nm in particular is of interest since light of that wavelength can excite an organic compound called protoporphyrin IX (PpIX) and make it fluoresce [25], and this compound is excreted by bacteria and can be a sign of an infection [26]. Sensors that aim to detect bacterial

presence through the fluorescence of PpIX should therefore be tested on phantoms made specifically for 405 nm.

Optical phantoms should mimic the major factors defining the interaction between tissue and light, namely the absorption coefficient and the reduced scattering coefficient [15]. They are both material properties that are dependent on the wavelength of light. The absorption coefficient (μ_a) is a measure of how far light of a certain wavelength can penetrate into a material before it gets absorbed by the material [5]. The reduced scattering coefficient (μ_s') is a measure of how light of a certain wavelength scatters within the material, and it is a composite measurement of the scattering coefficient (μ_s) and the anisotropy factor (g): $\mu_s' = (1 - g)\mu_s$ [15]. The scattering coefficient is the number of scattering events per centimeter, while the anistropy factor is the average cosine of the scattering angle [15]. Furthermore, refraction is the changing of the direction of light when it passes between different materials. Transmission is simply the let-through of light through a material without changing the direction of the light. Fig. 3.1 below illustrates these four kinds of light interaction.

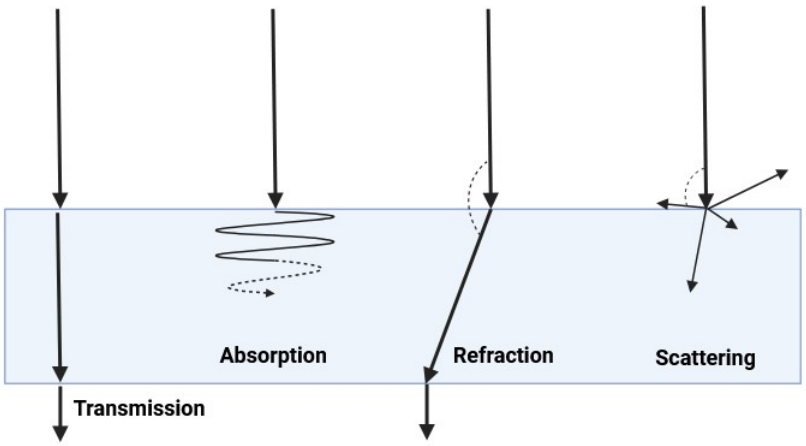

Figure 3.1: Schematic image showing four different ways that light can interact with a sample. Created in Biorender.com.

Scattering can not be measured in a simple spectrometric setup, and there is no single standard for measuring the reduced scattering coefficient in the field of optical phantoms [15]. Two common methods, however, are frequency domain photon migration (FDPM) and using integrating spheres. FDPM works by shining light of specific frequencies on a material and then detecting the resulting phase shift and amplitude reduction of the scattered light in the material, at a certain distance from the light source [27]. The other common option, generally seen as the best method for measuring phantom optical properties [15], is to use an integrating sphere connected to a spectrometer to get the transmission and reflectance spectra, which in turn can be used to calculate the relevant coefficients using IAD (inverse adding-doubling) [28, 29]. However, even this method using an integrating sphere often does not result in similar values between research groups, with discrepancies usually

between 10 and 15% and sometimes even up to 50% [15]. These discrepancies have been explained by a lack of standardization in phantom fabrication and a lack of model phantoms, as well as by differences in measurement systems [15].

Different methods are necessary for measuring absorption depending on if it can be assumed that no scattering is occurring, or not. If the sample has minimal scattering, absorption and absorbance can be assumed to be the same thing [5]. Absorbance measurements are simply measuring how much light is passing through a sample compared to a reference, so if no scattering is occurring, then all absorbance is due to the sample absorbing light. However, if the sample has substantial scattering properties, then the absorption can only be accurately measured simultaneously as the scattering, for example using one of the methods for measuring scattering mentioned above.

Optical phantoms are usually made using a matrix material, a scattering agent, and an absorbing agent [15, 16]. The choice of material should be made with the intended purpose of the resulting phantom in mind, as there are pros and cons of every material. In this thesis, PDMS will be used as the matrix, TiO_2 as the scatterer, and nigrosin as the absorber. PDMS, or polydimethylsiloxane, is a type of silicone. It is a cheap and semi-permanent matrix material, which makes it accessible and suitable for creating long-lasting phantoms [15]. The refractive index of PDMS is close to that of tissue (around 1.4 for both PDMS and *in vivo* tissue [15, 19]), which means that the raw material naturally interacts with light in a similar way to skin tissue. TiO_2, or titanium dioxide, is one of several metal-oxides commonly used as a scattering agent in phantoms [15, 16, 22]. It is stable in PDMS for several years [15]. TiO_2 also has a refractive index that is much larger than the refractive index of PDMS (around 2.4 to 2.9 for TiO_2, compared to 1.4 for PDMS), meaning that it is very potent as a scattering agent in this matrix material and can therefore create highly scattering phantoms [15, 19]. Nigrosin is a black synthetic dye that is one of several commonly used absorbing agents in optical phantoms [18, 28]. It exists in both alcohol- and water-soluble forms and can therefore be used with many different matrix materials. Nigrosin has a similar absorption spectra to human melanin over a large wavelength range [30], which makes it suitable for optical skin phantoms that work for more than one very specific wavelength.

The absorption and reduced scattering coefficients of tissue vary depending on a number of different factors. Tissue type, health status, age, and gender all affect the optical properties of tissue [31, 32]. The optical properties of skin are obviously greatly affected by skin colour, but the exact effects of skin colour on the optical properties of skin are severely understudied. The vast majority of studies on the optical properties of skin focus on fair skin colours, and most skin phantoms are made to mimic fair skin [6]. Only 1 % of studies about optical medical technologies even consider skin colour as a factor [5]. This has introduced a racial bias into these technologies, making them less sensitive and accurate for patients with dark skin tones [6]. In this study, the Fitzpatrick skin type (FST) model is used to cathegorise different skin colours, or more correctly, skin phototypes. It is the most widely used

skin colour cathegorisation model in research [6], even though it does not actually divide skin tones based on colour, but instead on how skin reacts to sun [5]. There are six FST types (I-VI), with type I being the fairest ("always burns, never tans") and type VI being the darkest ("always tans, never burns") [6, 24].

The phantoms developed in this thesis will be multi-layered to mimic the three main layers of human skin: the epidermis, the dermis, and the hypodermis (subcutaneous fat). Each skin layer has different average thicknesses and optical properties, all of which will be mimicked in the three different phantom layers. The layers will then be stacked on top of each other. The thickness of the skin layers vary from person to person and between different body parts, but the average thickness is about 0.2 mm for the epidermis [6, 32], 2.5 mm for the dermis [32], and several centimeters for the hypodermis [33], but the hypodermis can be assumed to be semi-infinite for this purpose. Most research studies on optical phantoms do not explain or reference how they got their target values for thickness and optical properties, which makes it difficult to verify the relevance of their chosen target properties. The target optical properties of each phantom layer in this thesis are however explained and referenced, and the values are based on studies on real human tissue, as shown in appendix *A3: Calculation of target optical properties*. Since the optical properties of individual skin layers can only be measured *in vitro* [9], i.e. on donated skin samples, the target optical properties used in this thesis will mostly be based on *in vitro* measurements. The measured absorption of skin will however differ depending on if it is an *in vivo* or an *in vitro* sample, mainly due to the presence of blood under the skin during *in vivo* measurements [11]. Furthermore, only the epidermis layer will have different optical properties for the dark- and fair-skinned phantoms, as most of the difference in optical properties between different skin colours is due to melanin in the epidermis [6, 24].

While single-layered optical phantoms have been made to mimic dark skin before [6], no articles on multi-layered phantoms for dark skin can be found. The benefit of creating multi-layered skin phantoms, especially when comparing phantoms for different skin colours, is that the phantom will mimic the combined optical properties of skin regardless of the penetration depth of the sensor. The reason why this is not the case for single-layered skin phantoms is because optical sensors on real human skin get a composite measure of the skin layers that is within that sensor's penetration depth, so the values will vary depending on how deep the sensor can measure [28]. With a single-layered phantom, however, the spectroscopic values will be the same regardless of penetration depth of the sensor. This especially becomes a problem when considering that the penetration depth is not only dependent on the sensor itself, but also on the optical properties of the sample. Optical sensors can measure deeper into fair skin than dark skin [5], which means that the optical properties of the underlying skin layers will affect the overall measurement more for fair than for dark skin. This means that a multi-layered skin phantom, where each layer mimics the optical properties of the real skin layer of interest, should show accurate spectroscopic readings regardless of the penetration depth that the sensor can manage in a specific condition and on a specific skin colour.

In summary, the research field of creating optical phantoms is rapidly growing but is as of yet lacking standardization in terms of materials, fabrication methods, measuring techniques, wavelength ranges, target optical values, and more, making it difficult to compare or confirm results. There is also a severe lack of studies that include different skin colours, especially darker skin tones. The unique contributions of this thesis include verifying and simplifying already published methods, creating phantoms for lower wavelength ranges, and creating multi-layered phantoms for both fair and dark skin.

3.2 Purpose

The aim is to develop a reliable method for creating optical phantoms for human skin. The skin phantom should be multi-layered to represent the epidermis, the dermis, and the hypodermis. Four versions of this phantom should be produced, so that they mimic fair skin at 405 nm, fair skin at 630 nm, dark skin at 405 nm, and dark skin at 630 nm, respectively. Each layer of each phantom version should have the same thickness and absorption coefficient (μ_a) as the respective human skin layer. They should be homogeneous and stable over time. The developed phantoms will be used by Odinwell for testing and calibrating their biosensor.

3.3 Research question

The main question that should be answered in this report is the following:

How can multi-layered optical skin phantoms be reliably produced in a laboratory setting?

Several sub-questions that clarify and specify the main question should also be answered:

- What production method will most reliably produce evenly thick phantoms of target thickness?
- What is the relation between the concentration of the absorbing agent and the absorption coefficient of the resulting phantoms?
- What are the necessary changes between the different phantom versions to mimic fair vs dark skin tones?
- What are the necessary changes between the different phantom versions to mimic skin at the wavelengths 405 nm vs 630 nm?
- Can porphyrin be incorporated and stable in PDMS phantoms to mimic the presence of bacteria in skin-like conditions?

3.4 Limitations

The phantoms will mimic the absorption coefficient but not the reduced scattering coefficient of human skin. This is because the available spectrometric instruments could not measure scattering, so while some experimentation to include a scattering agent into the phantoms is done, the scattering of the resulting phantoms is never measured. Furthermore, the aim is only to create an optical phantom, so the phantom will not be tuned to mimic other material properties of tissue, like the mechanical or acoustic properties.

The phantoms will only mimic the absorption of skin at a wavelength of 405 nm and 630 nm, respectively. The NIR and IR spectra will not be studied. No colorimetric analysis of the phantoms will be done either, so the phantoms will not mimic the colours and tones of human skin.

Any irregularities or inhomogeneities present in real skin - like pigmented spots, hair, and blood vessels - will also not be considered. This is because the purpose of the phantom is to have a stable and repeatable reference and therefore it has to be homogeneous.

4
Methods & Results

4.1 Experiments with RTV silicone

Some preliminary experiments were made with RTV (*room temperature vulcanizing*) silicone before the PDMS silicone arrived. The aims of these experiments were to test different steps and alternative methods of the phantom making process, as well as to practice the steps. RTV silicone was deemed a passable substitute since it, like PDMS, is a type of silicone often used in synthetic phantoms. The two materials are both tough, flexible, and hydrophobic, and they are both made up of a base and a hardener component, so the main PDMS phantom fabrication steps could be performed with RTV silicone too.

Methods

The basic process for creating the silicone phantoms was taken from Ayers et al [34], with some inspiration taken from Saager et al [28] and de Bruin et al [19]. It should however be noted that their processes were developed for PDMS, not RTV silicone. RTV silicone with hardness 15/Shore A (Make Make) with a base-to-hardener ratio of 100:3 was used for these experiments. The first step was to mix rutile TiO_2 powder (<5 μm, Sigma-Aldrich) into the hardener and put the mixture in an ultrasonic cleaner (model GS0203), stirring occasionally, for 30 minutes to break up clusters of TiO_2 particles. During this time the nigrosin solution (1% w/v alcohol-soluble nigrosin (Sigma-Aldrich) dissolved in either ethanol or isopropanol) was mixed into the elastomer base. The hardener solution and elastomer base solution were then mixed together. The silicone was then poured into molds of different materials and sizes. A sharp pin was used to pop any bubbles at the surface before the silicone started to cure. The silicone was fully cured within a few hours.

Five different molds were tested. Firstly, a 3D-printed well made entirely out of PLA (*polylactic acid*), similar to that described by Saager et al [28]. The used 3D-printer was an Original Prusa MK4S, and the designing process is described in more detail in section *4.2.1 Different types of molds*. Then rectangular edges or walls, like the previous mold but without a bottom, were also 3D-printed out of PLA. These walls were taped onto different materials to give them a removable bottom. The materials that were tested as removable bottoms were sanded PLA plates, microscope glass slides, and petri dish lids. Lastly, the bottom-less walls were also used as a divider between two microscopy glass slides, as described by de Bruin et al [19]. Different

depths (between 0.1 mm and 20 mm) and side lengths were also tested for the molds.

Three different methods were tested for achieving a smooth top surface for the phantoms. The first was to drag a palette knife over the top , as described by Saager et al [28]. The second was to press a glass slide down onto the mold so that the excess silicone spilled over, and then to slowly remove the glass by sliding it off the mold. For the double-sided glass mold, however, the silicone was simply left to cure between the two slides, with the divider in between to ensure the correct thickness, as described by de Bruin et al [19].

The phantoms were left to cure on either a still, flat surface, or in an ultrasonic cleaner for 30 minutes. This was done to test whether the air bubble content in the finished phantoms would be affected by curing in an ultrasonic cleaner.

Once the phantoms were cured, they were removed from their molds. They were visually assessed and their thickness was measured using a digital caliper. To create a multi-layered phantom, phantoms of different thicknesses were stacked on top of each other by adding drops of isopropanol to the top surface of the first phantom and then laying another phantom on top, similar to the stacking process of Greening et al [18]. Light pressure was added from above to remove any air bubbles from in between the layers.

Lastly, some experiments with incorporating porphyrin into silicone were also made. Different amounts of ethanol-dissolved protoporphyrin IX (Sigma-Aldrich) were mixed into the elastomer base during the phantom fabrication process (resulting in silicone with between 0.005 and 0.020 weight-% porphyrin), and the fluorescence of the resulting phantoms was assessed directly after curing and after a few days. The fluorescence was measured using a spectrometer, specifically Odinwell's developing biosensor, at the wavelength 405 nm.

Two methods of covering the porphyrin-containing phantoms were used in an attempt to increase the stability of the porphyrin. The first was to wrap the phantoms in laboratory plastic film (*Parafilm*) and the second was to cover the phantoms in a thin layer of pure RTV silicone. Some phantoms were left uncovered, as controls. The phantoms' fluorescence at wavelength 405 nm was checked directly after curing and after four days.

No other spectrometric tests were done on any of the RTV phantoms.

Results

Incorporating nigrosin into the elastomer base was quick and easy, whether the nigrosin was dissolved in ethanol or isopropanol. A few minutes of hand-mixing was enough to reach apparent homogeneity, and the mixture stayed homogeneous for the whole curing process.

The different molds affected the thickness, evenness, and surface texture of the resulting phantoms. The PLA mold, as well as the mold with the removable PLA bottom, resulted in a matte and slightly textured bottom surface that could affect the surface optical properties of the phantoms and result in air bubbles when stacked. The molds that used glass slides or petri dish lids as bottoms instead turned out completely smooth and shiny. The petri dish lids were however not completely flat but rather slightly concave, and this resulted in slightly uneven phantoms. The phantoms were easily removed from PLA and from the petri dish lids, but could get stuck very hard to the glass slides if left to cure overly long. Letting the phantoms cure in an ultrasonic bath worsened this problem, as the heat from the ultrasonic bath cured the silicone faster. The phantoms that had cured between two glass slides, with a divider in between, were however the hardest to remove. The removal often resulted in the breaking of the glass slides and ripping of the phantoms. The phantoms that were successfully removed from the double-sided glass molds were however very even and of the desired thickness, and both the top and bottom surfaces were unpatterned and shiny with the exception of air bubbles, since this method made it impossible to pop the bubbles at the surface before curing.

Air bubbles slightly deeper in the silicone was a problem for all phantoms, regardless of mold type or process. Only the thinnest phantoms (<0.3 mm) were completely rid of bubbles, as the thinness made it possible to pop all the bubbles from above before curing. The air bubbles appeared during the mixing of the elastomer base and the hardener, and since the silicone started to cure after just a few minutes, it was not possible to put the beaker with the silicone in an ultrasonic bath before pouring the silicone into the molds. The phantoms that were put into an ultrasonic bath while curing ended up having even more visible air bubbles than phantoms that were left to cure on a still, flat surface. This might be due to the ultrasonic vibrations bringing the air bubbles in the silicone to the surface, where they got stuck as the silicone cured. Silicone is often cured in vacuum chambers to draw out any bubbles, but I did not have access to a vacuum chamber and so could not test the effect of using one. The thinnest phantoms (0.2-0.3 mm) were also difficult to remove from all of the molds, as they often did not keep their structure and instead curled up into a tangled ball after being removed. This might be due to the 0.2 mm and 0.3 mm phantoms being too thin in places, as all of the phantoms that were cured in molds with a depth of 0.1 mm tore when they were removed.

The method for smoothing out the top surface of the phantoms before they cured affected the evenness of the phantoms. The thickness and evenness were measured using a digital caliper on different parts of each sample, which proved to be a precise and reliable method that did not indent or scratch the phantoms. The first method for smoothing out the top, to drag a palette knife over it, often made the top of the phantoms slightly concave - i.e. the surface was lower in the middle compared to at the edges - especially at the end from which the smoothing out started. The second method was to cure the silicone between two glass slides, which resulted in much more even phantoms, especially for the very thin phantoms ($\sim$0.2 mm). As mentioned earlier, the top surface was however disrupted by air bubbles to a high

degree and the glass slides were hard to remove. The third method was to press down with a glass slide onto the top surface and then slide it off the mold. This resulted in more even phantoms than using a palette knife, and had less air bubbles at the surface than using two glass slides.

The attempts at stacking layers of phantoms on top of each other by using drops of alcohol between each layer to avoid air bubbles were successful. The method proved to be simple and reliable.

The phantoms with porphyrin were not stable over time. Directly after curing, all porphyrin-containing phantoms fluoresced at around 650 nm when exposed to light of 405 nm. The fluorescence was completely gone after three days for all phantoms. This result is congruent with earlier findings by Pogue et al, which state that RTV silicone is not biologically compatible [15]. Covering the phantoms in either a plastic film or a thin layer of pure RTV silicone directly after curing did not increase the stability of the porphyrin in the samples, suggesting that air exposure is not the reason why the porphyrin deteriorated.

4.2 Experiments with PDMS silicone

Some of the experiments that had been done with RTV silicone were repeated with PDMS to check if the results were transferable. These experiments revealed several relevant differences between RTV silicone and PDMS. Cured PDMS is transparent while RTV silicone is an opaque white. PDMS cures much slower than RTV silicone - a 2-3 mm thick slab of RTV silicone cures in a few hours, while the same curing takes PDMS three days. This makes it much easier to avoid air bubbles in cured PDMS than RTV silicone, since the slow curing gives the air bubbles created during stirring and pouring time to rise to the top and pop at the surface. The slow curing of PDMS also makes it more prone to leaking out of molds during the curing process, in cases where the molds are not completely tight. Lastly, PDMS does not get stuck on glass once fully cured like RTV silicone does.

4.2.1 Different types of molds

Methods

Several different kinds of molds were tested to find which material and techniques resulted in the best phantoms in terms of thickness, evenness, repeatability, and lack of air bubbles.

Firstly, PDMS (Sylgard 184 Silicone Elastomer Kit, Dow Corning, with a base-to-curing agent ratio of 10:1) was cured on both microscope glass slides and on flat PLA plates to compare how easy the cured PDMS was to remove and how the bottom

surface of the PDMS would be affected.

After having tested different alternatives for the bottom surface, different kinds of wells (or the "walls" of the mold) were tested. 3D-printed PLA wells of different heights were either taped or glued to a bottom plate (see fig. 4.3), and then the PDMS was poured in and smoothed out with either a palette knife, or by pressing down with a glass slide and then carefully sliding it off sideways. For the thinnest layer, mimicking the epidermis (0.2 mm), a special tape well was also tested. This tape well was made by covering a glass slide with five layers of a clear, broad tape, creating a 0.2 mm thick stack of tape. A rectangular form was then cut out of the tape layers with a razor blade, creating a 0.2 mm deep well in the middle. All of the tape layers were cut through so that the underlying glass made up the bottom of the well, see fig. 4.4.

The 3D-printing of the PLA molds was done on an Original Prusa MK4S printer. The molds were first designed in the accompanying program PrusaSlicer, as seen in fig. 4.1. The molds were designed to be either 2.5 mm or 20 mm deep for the dermis and hypodermis layers respectively, but were otherwise identical. The outer measurements were 25 mm x 75 mm to fit perfectly on a microscopy glass slide, and the inner measurements of the well/hole was 15 mm x 30 mm, see fig. 4.2. This means that the phantoms produced in these molds would also have the measurements 15 mm x 30 mm, and be either 2.5 mm or 20 mm thick. The 3D-printer was set to 100% infilling to create as smooth a top and bottom layer as possible, which reduces the risk of leakage during phantom fabrication.

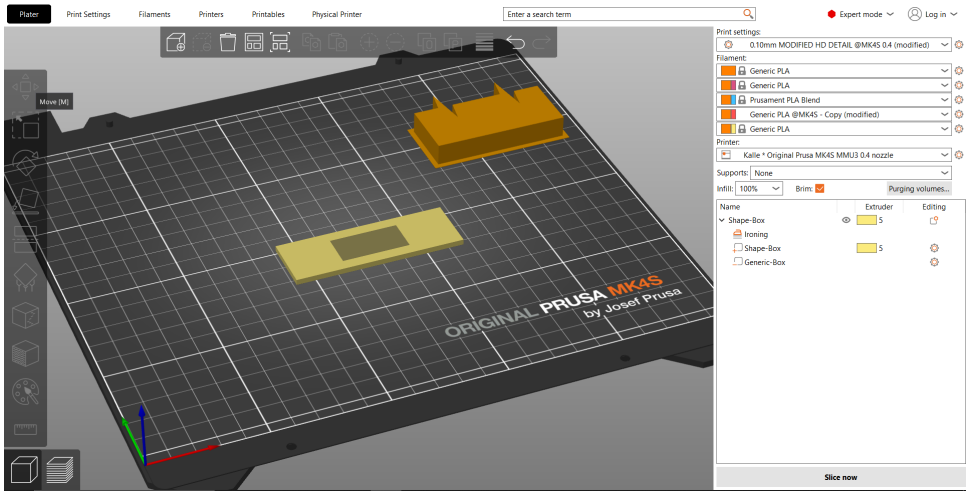

Figure 4.1: The layout in PrusaSlicer when designing objects for 3D-printing.

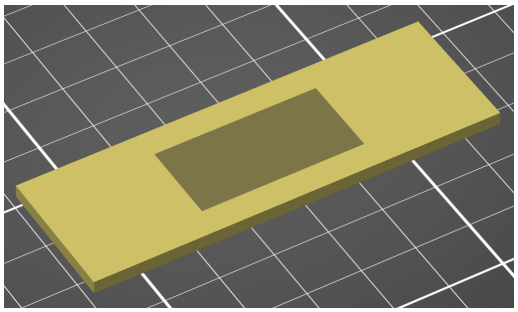

Figure 4.2: A close-up picture of the design for the 2.5 mm deep mold in PrusaSlicer. The dark rectangle in the middle of the structure is a hole that runs through the whole 2.5 mm mold.

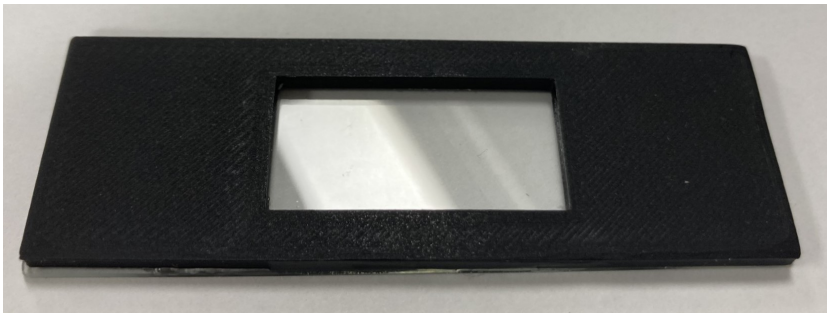

Figure 4.3: A 2.5 mm deep PLA mold glued to a microscopy glass slide.

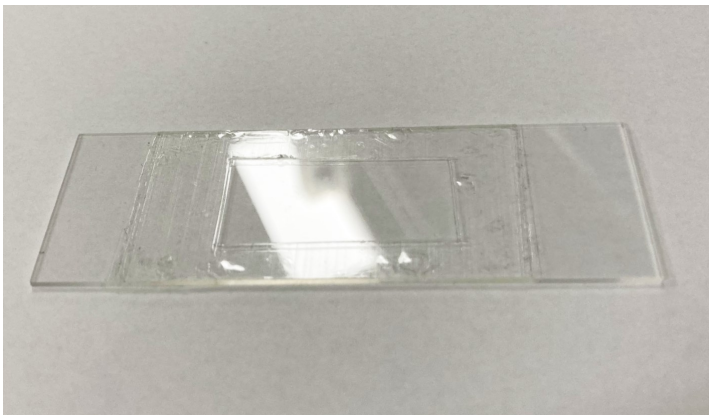

Figure 4.4: A 0.2 mm deep tape well on a microscopy glass slide for the epidermis layer.

Lastly, PDMS was also cured in a double-sided mold. This was created by either gluing a PLA well to or creating a tape well on a glass slide, pouring in the PDMS, and then placing a second glass slide on top. The excess PDMS was pressed out by pushing down on the top glass slide. The structure was then taped together to stabilize it. The finished double-sided molds were either left to cure on a flat surface, or tilted 45° on either the short or the long side.

The thickness of all cured samples was measured using a digital caliper, on three spots for each sample.

Alongside the testing of different molds, the use of the ultrasonic cleaner (model GS0203) was also tested by varying the length of time that the PDMS was left in the cleaner before it was poured into the molds. The tested lengths of time were between 5 and 30 minutes. The aim of this was specifically to check if the ultrasonic cleaner could help remove bubbles from the PDMS and if it would affect the curing process in any way.

Results

Using a glass microscope slide as the base for the molds resulted in a smooth, shiny, and unpatterned underside for the phantoms. Cured PDMS is also easy to remove from glass surfaces, in contrast to how RTV silicone sticks to glass once cured. Using a PLA plate as the base also made the cured PDMS easy to remove, but it resulted in matte and slightly patterned undersides.

For the molds with detachable bottoms, for example a PLA well simply taped to a glass slide, leakage during the curing process was common. The PDMS cured so slowly that even the smallest crack between the well and the bottom eventually led to a leak, which resulted in phantoms that were concave at the top and considerably thinner than intended. Gluing the well to the bottom plate solved this problem.

However, even the glued-down wells often resulted in phantoms that were too thin and had a concave top surface. This was not due to leakage but rather a result of smoothing out the top with a palette knife after having poured in the PDMS. Even though the knife was connected to both sides of the well, and thus never dipped into the mold, it still dragged more than just the excess PDMS with it. This might be due to the high viscosity of uncured PDMS. This also caused a slope in the phantoms, where the end that the smoothing had started at was a bit thinner than the opposite end. The issue of the sloping was slightly remedied by dragging the palette knife along the short sides of the mold instead of the long sides, thereby diminishing the length over which a slope could develop. The variation of thickness in a single sample, compared to the average thickness of the same sample, was $\pm 22\%$ for the thin (0.2 mm) phantoms and $\pm 8\%$ for the thick (2.5 mm) phantoms in one-sided molds. Regarding the average thickness, wells that were 2.5 mm deep produced phantoms that were up to 20% thinner than the target (i.e. the average thickness of each sample was between 2.0 mm and 2.5 mm), and wells that were 0.2 mm deep produced phantoms that differed up to $\pm 20\%$ of the target thickness (i.e. the average thickness of each sample was between 0.16 mm and 0.24 mm). See fig. 4.5 for an overview of the thickness data.

The unevenness of the phantoms was not helped by smoothing out the top by pressing down and then sliding off a second glass slide on top instead of using a palette knife, even though it resulted in more even phantoms when using RTV silicone. This

difference is probably due to material differences between PDMS and RTV silicone, as the uncured PDMS - unlike RTV silicone - tended to cling to the top glass slide, which made the whole process messy and uncontrolled. This method did not produce usable PDMS phantoms.

For the 0.2 mm phantoms, the tape wells proved to be better suited than the PLA wells. The tape wells had a more reliable depth than the PLA wells, since the thin PLA wells were easily warped while handled and glued down. Furthermore, the tape wells also made the removal of the phantoms from the glass bottom easier. The 0.2 mm phantoms often ripped when removed too quickly or when pulled from a single corner, but by using a tape well it was possible to remove the well itself from the glass before attempting to remove the phantom, thereby gaining access to the entire side lengths of the phantom.

Using the double-sided glass molds resulted in phantoms with low thickness variation in a single sample, varying by at most ±4% for the thin (0.2 mm) phantoms and ±5% for the thick (2.5 mm) phantoms. This was a much smaller variation than the one-sided molds managed. The average thickness of the 0.2 mm double-sided molds was up to 30% higher than target thickness (i.e. between 0.20 mm and 0.26 mm), and for the 2.5 mm double-sided molds it differed ±10% (i.e. between 2.25 mm and 2.75 mm). See fig. 4.5 for a side-by-side comparison of the different molds.

Target thickness:	0.2 mm		2.5 mm	
Type of mold:	1 glas	2 glasses	1 glas	2 glasses
Difference between target thickness & actual average:	(+/-) 20%	(+) 30%	(-) 20 %	(+/-) 10%
Average variation of thickness in a single sample:	0.088 mm	0.022 mm	0.24 mm	0.22 mm
Thickness variation in a single sample, relative average thickness:	(+/-) 22%	(+/-) 4%	(+/-) 8%	(+/-) 5%

Figure 4.5: The effect of different molds on the average thickness (expressed as a percentage of target thickness) and the thickness variation within a single sample (expressed as both the height difference between the thinnest and thickest point, and as a percentage of the average thickness). The data for the 0.2 mm molds were all from tape wells. The data for the 2.5 mm molds were all from glued-down PLA wells. The single-glas molds had all been smoothed out using a palette knife.

Opening the double-sided glass molds was difficult and often resulted in broken glass, since the PDMS had cured to both glass slides. The largest problem with the double-sided molds was however air bubbles, which could not escape due to the top glass slide. The bubbles were due to stirring and pouring the PDMS, or were created when the top glass slide was put in place. This meant that when left to cure on a flat surface, phantoms in double-sided molds ended up with numerous air bubbles all over the surface. The attempts to let the air bubbles rise to a specific side by tilting the molds 45° during curing were not entirely successful. Most air bubbles did rise to the upward-pointing side, leaving the rest of the phantom clear, but in most cases new air bubbles would rise from the bottom side. This was probably due to some small cracks between the top glass slide and the top of the well that

let in small amounts of air. These air bubbles could be scattered all over the cured phantoms.

It should be noted that, in contrast, air bubbles did not appear in the cured phantoms of any of the one-sided molds. Air bubbles in the uncured PDMS of one-sided molds could be popped from above with a sharp pin, or would pop by themselves when they reached the surface. This held true even when the PDMS contained a lot of air bubbles when poured into the mold, for example because the PDMS had just been stirred or had only been in the ultrasound bath for a short time.

The effect of the time that the uncured PDMS was left in an ultrasonic cleaner after the curing agent was mixed in with the elastomer base was also studied. The longer the PDMS was left in the cleaner, the fewer bubbles were left in the PDMS, which was the purpose of using the ultrasonic cleaner. However, the steadily increasing heat from the ultrasonic cleaner would hasten the curing process and make the PDMS thick and tough at the bottom and sides of the container. This made it difficult to pour the PDMS into a mold. 15 minutes in the ultrasonic cleaner turned out to be a good compromise where almost all of the bubbles were gone but the cleaner had not yet become hot enough to significantly start curing the PDMS.

Appendix *A1: Protocol for optical phantoms (one-sided mold)* and *A2: Protocol for optical phantoms (double-sided mold)* contain the modified protocols for one- and double-sided molds, respectively. These protocols are based on the findings from this section of the report.

4.2.2 Optical properties

The only optical property that was measured was absorption for the wavelengths 405 nm and 630 nm. While scattering was not measured, the incorporation of the scattering agent titanium dioxide (TiO_2) into phantoms was tested to find the best method for adding it.

Methods

The target optical properties of each phantom layer was calculated using previous studies presenting the μ_a and μ'_s coefficients of real skin tissue, as described in appendix *A3: Calculation of target optical properties*. The necessary concentrations of alcohol-soluble nigrosin (Sigma-Aldrich) and rutile TiO_2 powder (<5 μm, Sigma-Aldrich) to reach these target values were roughly estimated using a study by Greening et al [18], which presents the resulting absorption and reduced scattering coefficients of PDMS phantoms with different concentrations of nigrosin and TiO_2, between the wavelengths 591 nm and 851 nm [18]. Due to the limited wavelength range and the limited μ_a and μ'_s values presented in the Greening et al study, the recommendations in the study had to be heavily extrapolated from and were only used as vague indications of what the appropriate concentrations of the two agents

might be for the different phantom layers.

The incorporation of these agents was first done as described by Ayers et al [34] and at the estimated appropriate concentrations. This meant that the nigrosin/ISO solution was mixed in with the elastomer base while the TiO_2 was mixed in with the curing agent and put in an ultrasonic bath for 30 minutes, before the two solutions were mixed together. An alternative method, namely mixing in both the nigrosin/ISO solution and the TiO_2 with the elastomer base and then putting it in an ultrasonic bath, was also tested. Different concentrations of the nigrosin/ISO solution were tested to see the impact of ISO on the curing process and finished phantoms.

The effect of different concentrations of nigrosin on the absorption coefficient was then determined by measuring the absorbance of phantoms without any TiO_2 but with differing concentrations of nigrosin (between 5 and 200 μl of 1% nigrosin/ISO per gram of PDMS). Three samples were made for each concentration to account for batch effects. The phantoms were all 2.5 mm thick and made according to the protocol in appendix *A2: Protocol for optical phantoms (double-sided mold)*, with double-sided glass molds. At first, the phantoms were kept in their molds during the spectroscopic measurements to enable a stable setup for the samples. The reference for these measurements was an empty double-sided glass mold with 2.5 mm between the two glasses. Another round of measurements was then made directly on the phantoms, once they had been removed from their molds (see fig. 4.6). The reference for these measurements was a 2.5 mm sample of pure PDMS.

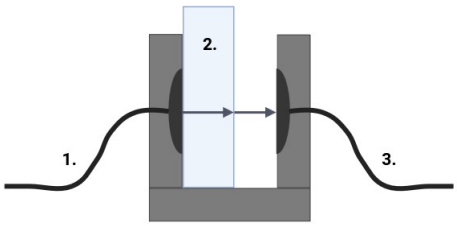

Figure 4.6: A side view of the spectroscopic setup.
(1. Optic fiber emitting light. 2. PDMS sample. 3. Optic fiber receiving light.) Created in Biorender.com.

The absorbance of these phantoms was measured using a specific spectrometric setup (see fig. 4.7). A DC power supply was connected to a diode that emitted light of either 405 nm or 630 nm. The diode was in turn connected to an optic fiber that was placed in a secure setup with the opposite end against the sample. A second optic fiber received the light that passed through the sample, and this fiber was connected to a benchtop spectrometer. The spectrometer then gave the absorbance for 405 nm or 630 nm, depending on which diode was used. Each phantom was measured on three different spots to verify the results and to detect any spatial variance in absorbance within a single sample. The absorbance was then converted

to an absorption coefficient, see an example calculation in appendix *A4: Example calculation of* μ_a.

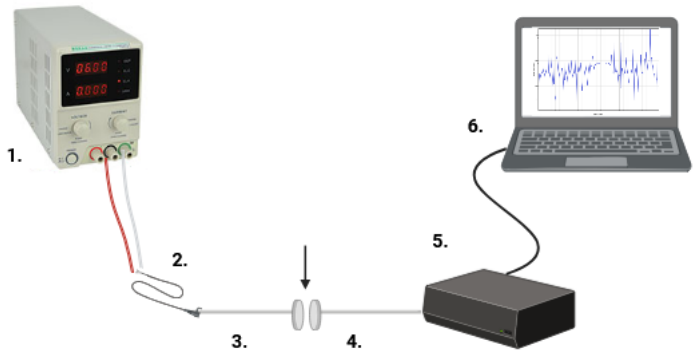

Figure 4.7: A schematic image of the spectrometric setup. The arrow shows where the sample goes.
(1. DC power supply. 2. Diode for 405 nm or 630 nm. 3./4. Optic fibers (stabilized so they would not move). 5. Benchtop spectrometer. 6. Computer showing absorbance measurements.)
Created in Biorender.com.

Using the resulting relation between the nigrosin concentration and the absorption coefficient, all necessary phantom layers were then made using the appropriate nigrosin concentrations. The phantom layers were made in both the correct thickness (i.e. 0.2 mm for epidermis, 2.5 mm for dermis, and 2 cm for hypodermis), as well as in an extra 2.5 mm thick sample for easy spectrometric measuring. Three batches were made for each phantom layer. Their absorption was measured spectrometrically on three different spots on each sample.

Lastly, to investigate the optical interface effect of stacking phantom layers on top of each other, an epidermis layer was lain atop a dermis layer and the combined absorption of the two layers was measured. The stacking was performed by first adding two drops of isopropanol on the dermis layer and then putting down the epidermis layer on top, in order to prevent air bubbles from being stuck between the two layers. Both layers had been bathed in isopropanol before the stacking to ensure that no dust would get trapped between the layers. Fig. 4.8 shows an epidermis layer stacked on a dermis layer. The absorbance of each layer individually as well as the combined absorbance of both layers were measured spectrometrically, to investigate the effect of the interface on the combined absorbance.

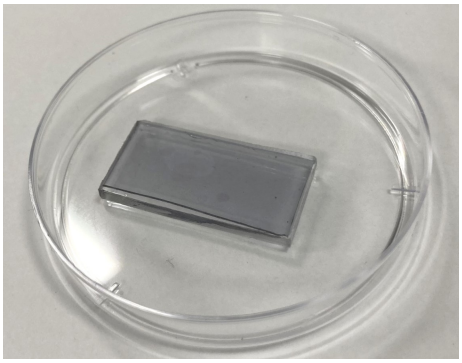

Figure 4.8: Two stacked phantom layers, with the epidermis layer on top of the dermis layer. Both layers are made to mimic the absorption of a 630 nm phantom for fair skin.

Results

The 405 nm phantom layers require much more nigrosin and TiO_2 than the 630 nm phantom layers to reach the natural optical properties of human skin, due to skin being more absorptive and scattering at 405 nm than 630 nm, see appendix *A3: Calculation of target optical properties*. Furthermore, the epidermis layers require a lot more nigrosin and TiO_2 than the other layers, and this is especially true for the dark epidermis (FST V-VI). The 405 nm dark epidermis layer is therefore the layer that requires the largest concentrations of nigrosin and TiO_2.

When incorporating the estimated necessary amounts of nigrosin/ISO and TiO_2 in the method suggested by Ayers et al [34], some problems arose for the layers that required high concentrations of the two agents. Firstly, the isopropanol that the nigrosin is dissolved in can react with the PDMS. At concentrations equal to or higher than 100 μl ISO per 1 gram of PDMS, the silicone does not cure completely, or at all. The two materials can also separate slightly and cause colour variations. This can be avoided by using a more concentrated nigrosin/ISO solution for highly absorptive layers than the 1% solution that is suggested by Greening et al [18]. However, highly concentrated nigrosin/ISO solutions will sometimes not dissolve all of the nigrosin and result in visible specks of nigrosin powder, so the solution should therefore not be more concentrated than is necessary to keep below the limit of 100 μl ISO per 1 gram of PDMS. High-concentration solutions of nigrosin/ISO should be sonicated for 10 minutes to break up any clumps. For phantoms with very high concentration of nigrosin, above circa the equivalent of 500 μl of 1% nigrosin/ISO per gram of PDMS, the PDMS does not cure properly even with the precaution of using a more concentration nigrosin/ISO solution. This suggests that the nigrosin itself, and not just the isopropanol, hinder the curing at large enough concentrations.

The second issue occurred when trying to incorporate high concentrations of TiO_2 into PDMS. Ayers et al [34] suggest mixing in the TiO_2 with the curing agent and then putting that solution into an ultrasonic bath for 30 minutes, before mixing it in with the elastomer base. This method worked well and resulted in evenly coloured

phantoms without visible clumps of TiO_2, but only for phantoms with a low concentration of TiO_2. For both epidermis layers at 405 nm, the estimated amount of TiO_2 was too large to mix in to the curing agent, as the curing agent mixture became too thick and saturated to dissolve the TiO_2 powder. The alternative method of mixing in the TiO_2 into the elastomer base and putting that mixture into the ultrasonic bath for 30 minutes, before mixing in the pure curing agent, was much more effective for high TiO_2 concentrations. It resulted in phantoms with a completely even distribution of TiO_2 and no visible particles. This alternative method therefore worked better than the original method for high concentrations of TiO_2, and worked as well as the original method for low concentrations of TiO_2. There were no negative side effects.

As mentioned in the *Methods* section above, the absorbance of the phantoms without any TiO_2 and with differing concentrations of nigrosin was measured in two different ways: first while they were still in their double-sided glass molds, and then once they had been removed from their molds. The results from the measurements done through the glass molds can be disregarded due to a systematic error, namely the choice of reference. This issue became apparent when the phantoms with low concentrations of nigrosin (15 μl/g of 1% nigrosin/ISO or less) showed up as having negative absorbance, meaning that they let through more light than the reference did. The reference was as mentioned an empty double-sided glass mold, meaning that the light traveled through two glass plates with 2.5 mm of air in between. It is obviously unreasonable that air should absorb more light than PDMS that has been dyed a faint grey, suggesting that an empty double-sided glass mold was not an appropriate reference. This will be discussed more in section *5. Discussion*.

The absorbance measurement that were done on the very same phantoms, but removed from the molds (see fig. 4.6), did not have the same issue, as all values were positive. The absorbance measurements for all phantoms were converted into absorption coefficients (see appendix *A4: Example calculation of* μ_a) and the results are shown in fig. 4.9. The data from fig. 4.9 is plotted in fig. 4.10.

Conc. 1% nigrosin (µl/g)	μ_a for 405 nm (cm^{-1})	μ_a for 630 nm (cm^{-1})
5	0.47	0.90
15	1.25	2.32
20	2.24	3.62
25	2.68	4.20
35	2.04	3.50
50	4.27	6.25
75	8.05	11.31
100	7.02	8.88
150	11.3	14.15
200	13.36	16.48

Figure 4.9: Average measured absorption coefficients of PDMS with different concentrations of 1% w/v nigrosin/ISO, at 405 nm and 630 nm.

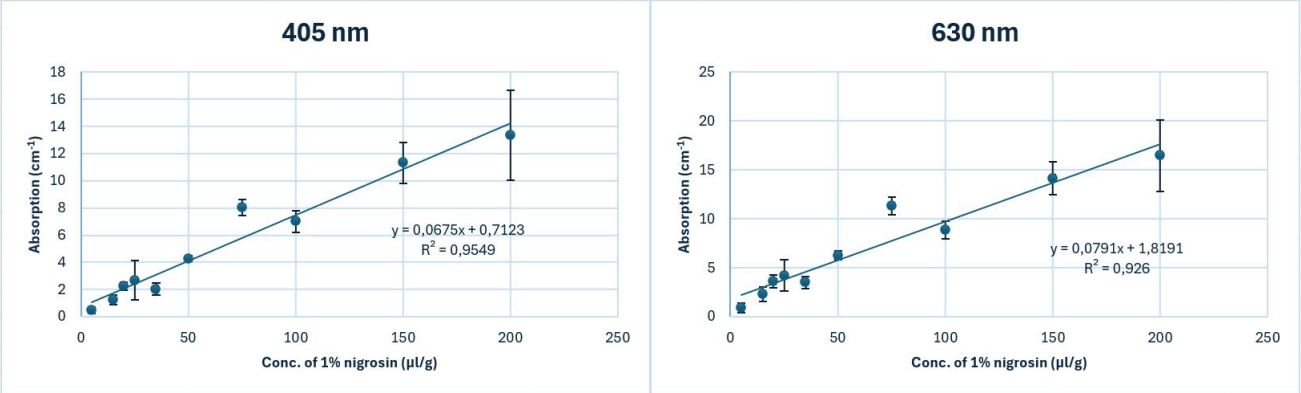

Figure 4.10: The absorption coefficient is plotted as a function of the nigrosin concentration, with data from fig. 4.9.

As shown in fig. 4.10, there is a clear positive linear relation between the concentration of nigrosin and the absorption coefficient (μ_a) in PDMS phantoms. The best fit for these two relationships, for 405 nm and 630 nm, are the following:

$$\mu_{a,405nm} = 0.0675 * C_{1\%nig/ISO} + 0.7123 \tag{4.1}$$

which can be rearranged to:

$$C_{1\%nig/ISO} = \frac{\mu_{a,405nm} - 0.7123}{0.0675} \tag{4.2}$$

and

$$\mu_{a,630nm} = 0.0791 * C_{1\%nig/ISO} + 1.8191 \tag{4.3}$$

which can be rearranged to:

$$C_{1\%nig/ISO} = \frac{\mu_{a,630nm} - 1.8191}{0.0791} \tag{4.4}$$

where:
$\mu_{a,\ 405\ nm}$ = the absorption coefficient for 405 nm [cm^{-1}],
$\mu_{a,\ 630\ nm}$ = the absorption coefficient for 630 nm [cm^{-1}],
$C_{1\%\ nig/ISO}$ = the concentration of 1% w/v nigrosin/ISO [μl/g].

Using eq. 4.2 and 4.4, the necessary concentration of 1% w/v nigrosin/ISO to reach a specific absorption coefficient for 405 nm and 630 nm, respectively, can be calculated. This was done with the μ_a target values of each phantom layer, the results of which are shown in fig. 4.11. The calculated necessary concentrations for the 630 nm dermis and hypodermis layers are listed as 0 μl/g in fig. 4.11, even though eq. 4.4 gives that a target μ_a of 0.7 cm^{-1} should result in a 1% nigrosin concentration of -14 μl/g. Since a negative concentration is not actually possible, the result was substituted with a zero. The fact that the equation predicts the need for a negative concentration of nigrosin to reach any μ_a below 1.8 cm^{-1} points to an issue with the equation itself. One likely explanation is that the equation is just not precise enough and would need more data points to improve the accuracy, especially at low concentrations of nigrosin. As seen in fig. 4.9, a sample with a 1% nigrosin concentration of 5 μl/g resulted in a μ_a of 0.90 cm^{-1} at 630 nm, so it should be possible to get positive absorption values for samples with a nigrosin concentration lower than 1.8 μl/g. One source of unwanted variation in the data behind the equation might also be the concentration of the nigrosin/ISO solutions that were used in the different samples. Since the ISO prevented the curing of PDMS at concentrations above 100 μl ISO per 1 gram of PDMS, more concentrated nigrosin/ISO solutions had to be used for samples that needed a high nigrosin concentration. These more concentrated nigrosin/ISO solutions were however not ideal for dissolving the nigrosin, accidentally resulting in samples with too low nigrosin concentrations. This can be seen in fig. 4.10, where the data point for 75 μl/g has higher absorption than the data point for 100 μl/g does. This is because a 1% nigrosin/ISO solution was used for the 75 μl/g samples while a 5% nigrosin/ISO solution was used for the 100 μl/g (and higher) samples.

Phantom layer and wavelength:	Target μ_a (cm^{-1})	Conc. 1% nigrosin (µl/g)
Hypodermis, 405 nm	6.2	81
Hypodermis, 630 nm	0.7	0
Dermis, 405 nm	4.3	53
Dermis, 630 nm	0.7	0
Epidermis (fair), 405 nm	23.9	344
Epidermis (fair), 630nm	6.8	63
Epidermis (dark), 405 nm	55.4	810
Epidermis (dark), 630 nm	15.7	175

Figure 4.11: The concentration of 1% w/v nigrosin/ISO necessary to reach the target μ_a for each PDMS phantom layer, calculated using eq. 4.2 and 4.4.

Each phantom layer, for both 405 nm and 630 nm, were made in two batches and each batch made two samples, one of which was 2.5 mm thick while the other one had the target thickness of that layer (0.2 mm for epidermis, 2.5 mm for dermis, and 20 mm for hypodermis). The absorption measurements, the results of which can be seen in fig. 4.12 and 4.13, were made on the 2.5 mm samples to facilitate the measurements. Three different phantom layers are absent from the results in fig. 4.12 and 4.13, namely the 405 nm dark epidermis layer and the 630 nm dermis and hypodermis layers. The missing results from the two 630 nm layers is due to them being fabricated without any nigrosin at all, as explained above. Their absorption could not be meaningfully measured, since the reference setup was a pure PDMS sample - i.e. the exact same thing as the produced 630 nm dermis and hypodermis layers. These measurements therefore only resulted in noise. The 405 nm dark epidermis layer had the different problem of containing too much nigrosin. Despite several attempts at creating this layer, trying different concentrations of the nigrosin/ISO solution to keep the ISO-to-PDMS ratio down, the samples did not cure properly and instead remained sticky. This points to there being a limit to the concentration of nigrosin that PDMS can contain while still curing, regardless of the ISO that the nigrosin is dissolved in.

The μ_a of the rest of the phantom layers, which were made and measured successfully, differed with between 7 and 18% from the target μ_a. All layers except the 630 nm dark epidermis had a higher μ_a than desired.

405 nm	Epidermis (fair)	Epidermis (dark)	Dermis	Hypodermis
Target μ_a (cm^{-1})	23.9	55.4	4.3	6.2
Actual μ_a (cm^{-1})	26.9	-	4.7	7.3
Difference	(+) 13%	-	(+) 9%	(+) 18%

Figure 4.12: Target vs measured μ_a for each 405 nm phantom layer.

630 nm	Epidermis (fair)	Epidermis (dark)	Dermis	Hypodermis
Target μ_a (cm^{-1})	6.8	15.7	0.7	0.7
Actual μ_a (cm^{-1})	7.6	14.6	-	-
Difference	(+) 12%	(-) 7%	-	-

Figure 4.13: Target vs measured μ_a for each 630 nm phantom layer.

The absorption of the stacked epidermis and dermis layers was also measured, see fig. 4.14. The absorption for the stacked layers was higher than what would be expected from just combining the absorption of the two layers individually, with the smallest difference being for the 405 nm fair phantom (+30%) and the largest for the 630 nm fair phantom (+100%). It is expected that the percentual difference is smallest for the phantom with the most absorptive layers, since the interface effect should be very similar in absolute terms regardless of the μ_a of the layers. The effect is however very substantial for all stacked layers.

Average μ_a (cm^{-1})	Epidermis	Dermis	Epidermis + dermis	
			Expected	Measured
405 nm (fair)	26.0	5.0	6.5	8.5
630 nm (fair)	8.5	0	0.6	1.2
630 nm (dark)	12.3	0	0.9	1.5

Figure 4.14: The measured μ_a for different phantom layers separately as well as when stacked together.

5
Discussion

This report started with a literature study to figure out the best optical model for healthy skin, taking a list of requirements into account. The study resulted in a decision to create a synthetic optical phantom with multiple layers, made out of PDMS and with nigrosin and TiO_2 as the absorbing and scattering agents, respectively. This was the easiest and most stable alternative and could be made homogeneous and accurate to the optical properties measured on skin in previous studies. Using nigrosin as the absorbing agent did however turn out to be limiting for achieving very high μ_a values, which will be discussed later on.

One negative side effect of using a synthetic phantom instead of a model based on a tissue sample is that it is necessary to have set target optical properties prior to creating the model. Deciding and calculating these target values involved a fair amount of assumptions and uncertainties. For example, *in vivo* and *in vitro* optical measurements of skin vary significantly, but skin layers can only be measured separately *in vitro*. I therefore based the target properties for each skin layer on the spectrometric measurements of *in vitro* Asian skin samples by Shimojo et al [35]. I assumed that these samples corresponded with FST III-IV, and used *in vivo* spectrometric measurements by Setchfield et al [5] on skin of different FST categories to adjust the target properties of the epidermis to those of FST I-II and FST X-IV individuals. This was done by assuming that the differences in optical properties were only due to melanin in the epidermis. Using different approaches and assumptions may result in widely different target properties. Different studies on the optical properties of skin also report a large variation of values, so just using other sources may give a different result. No other studies that I have found on optical skin phantoms have been transparent about the sources or assumptions they have used to reach their target properties, which makes this report have a unique contribution in that. Furthermore, this report is also unusual in the optical phantom field due to its focus on creating skin phantoms that mimic dark skin, and generally skin at the relatively short wavelength of 405 nm. Making 405 nm phantoms presents particular challenges in reaching the high μ_a and μ'$_s$ values that skin has at that wavelength.

The first step of the laboratory experiments was to investigate what process was best suited for fabricating the phantoms. The aim was to test previously established methods from earlier publications in a comparative manner, as well as to simplify them and make them work for the available laboratory equipment. Repeatability and simplicity was prioritised.

The basic steps of the process was inspired by Ayers et al [34], but with the exception of using the molds described in the articles by Saager et al [28] and de Bruin et al [19], since Ayers et al did not control for the exact height of their phantoms. The 3D-printed wells used in this thesis were similar to the wells used by Saager et al, but their results were not quite replicated here. Saager et al do not mention any issues with the bottom surface of the phantoms becoming patterned, presumably because the unspecified material of their wells was completely smooth. This was however not the case with the 3D-printed wells tested in this thesis. Glass was the only material tested that resulted in completely unpatterned and shiny bottom surfaces of the phantoms, which is why a new kind of mold was developed, with a hollow 3D-printed well and a detachable bottom made out of a glass microscope slide. The importance of having smooth surfaces on the phantoms is because of two different reasons. Firstly, having smooth surfaces enables the tight stacking of phantom layers without any crevices for air between the layers, which would create optical inhomogeneities in the finished multi-layered phantom. Secondly, rough surfaces would cause more scattering of light at the interfaces and make the optical properties less controllable.

Using the method with the one-sided wells suggested by Saager et al resulted in substantial issues with thickness and evenness. The average thickness of a phantom layer could not be exactly controlled, and the magnitude of this problem seems to be similar between this thesis and the Saager et al article, as the thinnest phantoms could vary tens of microns in both reports. The spatial variance, here defined as the percent deviation from the mean thickness, was also an issue, and averaged about $\pm 22\%$ for 0.2 mm phantoms in one-sided molds. Saager et al do not report on the frequency, size, or nature of the spatial variance in their experiments, but in this thesis, almost all of the spatial variance exists because of the height difference between opposite ends of the phantoms, not because of random irregularities.

The spatial variance was much reduced by the double-sided mold developed by de Bruin et al [19], reaching $\pm 4\%$ for the 0.2 mm phantoms and $\pm 5\%$ for the 2.5 mm phantoms. The two major drawbacks of this method, neither of which are mentioned by de Bruin et al, are the removal process of the cured phantoms and the problems of leakage and air bubbles. Removing the phantoms from between two slides of glass was difficult and time-consuming, and often led to the glass breaking. Eye protection is recommended for this process. Air bubbles in the finished phantoms was also a constant issue, as they would be distributed over the entire top surface when the phantoms were left to cure on a flat surface, as suggested by de Bruin et al. This problem can not be fixed by simply leaving the uncured PDMS in an ultrasonic bath for longer, as bubbles would appear when the second glass slide was laid on top of the mold even when the PDMS previously was completely free of bubbles. Air bubbles would also appear after the second glass slide was added, due to small gaps between the well and top glass slide that leaked PDMS and/or let in air. No solution for preventing or removing the air bubbles was found, but the problem was managed somewhat by letting the phantoms in double-sided molds cure at a 45 degree angle. This caused the air bubbles to rise and congregate at one

side of the mold and resulted in phantoms where most of the bottom portion was free of air bubbles.

To summarise, there are clear pros and cons for both kinds of molds, and your choice between the two molds should be based on what the intended purpose of the phantom is. The double-sided mold is preferable if low spatial variability is prioritised and if only point measurements are going to be made, since it is difficult to create larger areas of bubble-free phantoms with this process. The one-sided mold is preferable if whole phantoms without point irregularities (like small air bubbles) are required. The one-sided mold is also preferable for all phantoms that are supposed to be single-layered and semi-infinite, since the exact thickness and spatial variance of thickness is completely irrelevant in those cases. In this thesis, I chose to use the one-sided mold for all layers of the final phantom due to prioritising the wholeness and lack of air bubbles that it provides. I however chose to use the double-sided molds for determining the absorption of PDMS with varying amounts of nigrosin, since the low spatial variability made the spectrometric measurements easier and more repeatable.

One aim of this project was to simplify the phantom fabrication process and to work within the limits of the available laboratory equipment. One such limit was that I did not have access to a vacuum chamber, which is often used for the purpose of removing air bubbles from silicone while it is curing. This seems to be the standard procedure when working with silicone in the phantom research field. Here, other alternatives - like an ultrasonic bath, popping bubbles with a sharp pin, or simply leaving the PDMS to cure undisturbed - were tested instead. A notable difference between a vacuum chamber and an ultrasonic bath is that ultrasonic baths emit an increasing heat during running, and this hastens the curing of PDMS. Using the ultrasonic bath for only a limited amount of time before pouring the PDMS into the molds turned out to be a good compromise, as it was effective at removing bubbles but did not have time to heat the PDMS significantly. Once the PDMS had been poured into the molds, there was no need for an additional step of air bubble removal as the bubbles rose to the surface and popped by themselves long before the PDMS had time to cure. This result shows that silicone phantoms can be made even without the use of a vacuum chamber.

While this thesis does not include measurements of the scattering properties of the phantoms, the incorporation of the scattering agent TiO_2 was still tested. Ayers et al suggested mixing the TiO_2 with the curing agent and using an ultrasonic bath to break up any clumps of TiO_2 [34]. This worked well for low concentrations of TiO_2, but for higher concentrations there simply was not enough curing agent to dissolve the TiO_2 in. Instead, mixing the TiO_2 directly with the elastomer base and then putting that mixture in an ultrasonic bath was much more successful for high concentrations of TiO_2. There were no visible clumps of TiO_2 in the cured phantoms when this alternative method was used. This process is especially useful when producing optical phantoms for highly scattering tissues, like the epidermis, and for shorter wavelengths of light, like 405 nm. This is because more TiO_2 is required

to reach the higher reduced scattering coefficients needed for shorter wavelengths. Since most articles that have been published on optical skin phantoms focus on mimicking the optical properties for NIR or IR light, this mixing in of TiO_2 does not to seem to have been an issue for other researchers.

Nigrosin dissolved in alcohol was used as the absorbing agent, as is common for PDMS-based phantoms. The need to create highly absorbing phantoms, due to mimicking dark skin at a low wavelength, created unique problems that other researchers in the field have not reported on. The first problem was regarding the effect of ISO on the curing of PDMS. This effect started at 100 μl ISO per 1 gram of PDMS, so to keep below that limit, higher concentrations of the nigrosin/ISO solution had to be made for highly absorbing samples. These solutions had to be sonicated for 10 minutes to break up any clumps of nigrosin before being added to the PDMS. Even this measure was not enough to fully dissolve and distribute the nigrosin equally in the ISO solution, as samples that used different concentrations of nigrosin/ISO solutions seemed to end up with slightly inconsistent μ_a values. This was probably because some of the nigrosin in the more concentrated nigrosin/ISO solutions settled at the bottom of bottle and left the rest of the solution less concentrated, making the samples that it was used in contain too little nigrosin. The second problem with incorporating nigrosin into PDMS was regarding the nigrosin itself hindering the curing of PDMS, regardless of the amount of ISO. Nigrosin seems to stop the curing of PDMS at concentrations of around 6 mg per gram of PDMS and higher. This puts a limit on how high nigrosin can make the μ_a coefficient of a PDMS phantom.

The relation between the nigrosin concentration and the absorption coefficient was then determined by measuring the absorbance of phantoms with differing concentrations of nigrosin. At first, the spectrometric measurements were made through the double-sided glass molds, but this resulted in negative absorbance values for some samples. This means that these samples let through less light than the reference, which was an empty double-sided glass mold. The issue with this way of measuring was probably that the difference in refractive index between glass and air is bigger than that between glass and PDMS. When light travels from one material to another, some of the light will scatter at the surface of the second material. The bigger the difference in refractive index between the two materials, the more light will scatter. The refractive index of air is about 1, for PDMS it is about 1.4 [19], and for glass it is somewhere between 1.4 and 1.7 [36]. So when light travelled through the reference, it hit glass, then air, and then glass again, and the difference in refractive index between glass and air meant that a lot of light was scattered at both interfaces. More light could pass through the samples just because the difference in refractive indices is smaller for glass and PDMS. This meant that the measured absorbance for all samples was lower than it should be, and in some cases even negative.

Therefore, the samples were all measured again, without the glass molds. These results showed a positive linear relation between the nigrosin concentration and the μ_a for both 405 nm and 630 nm. These relations were then used to calculate the

necessary concentrations of nigrosin to reach the target properties of each phantom layer. This became problematic for three different layers: the 405 nm dark epidermis, and the 630 nm dermis and hypodermis layers. The 405 nm dark epidermis required too much nigrosin to cure, which suggests that another absorbing agent entirely would be needed to produce this layer. This would need to be further researched in the future by trying different absorbing agents, as no previous studies have tried to mimic such high μ_a coefficients for such low wavelengths. The 630 nm dermis and hypodermis layers, on the other hand, had very low target μ_a coefficients. The equation relating the nigrosin concentration to the 630 nm μ_a coefficient thus indicated that the nigrosin concentration would have to be negative in order to reach the target μ_a, which of course is impossible. This suggests that the equation is not accurate in the lower ranges, a problem that could probably be solved by further investigating the 630 nm relation between the very low concentrations of nigrosin and the resulting μ_a coefficient.

The interface effect of stacked layers on the absorption of a combined, multi-layered phantom should also be studied further, as it turned out to significantly increase the μ_a coefficient. One way of counteracting this effect would be to make each phantom layer slightly less absorptive than what the target for that layer actually is, so that the combined absorption of the multi-layered phantom will not be too high once the interface effect is taken into account. Studying any possible interface effect between the layers of real human skin would also be interesting to have a relevant comparison and target.

As a summary, I will now compare the results to the stated goals from the project specification. The first goals were to create a relevant substitute to healthy human skin, with the relevant optical properties for 405 nm and 630 nm. The created phantoms have essentially achieved this in terms of the thicknesses and μ_a coefficients for each layer, but falls short in mimicking the μ'$_s$ coefficient and in mimicking the absorption for the 405 nm dark epidermis layer as well as for the stacking of several layers. The next goals were to create stable and homogeneous phantoms. The phantoms should be stable for at least a few years, and they have homogeneous optical properties but some significant variation in thickness, so this is a partial success. The next goal, to develop a cheap and easy method of creating the phantoms, is however fully achieved. The process presented in this report is thoroughly tested and described, and possible to perform even with very limited laboratory equipment. The last goal was to create a stable porphyrin model, but this was not achieved as PpIX is not stable in the chosen matrix material.

6
Conclusion

A modified and simplified method, based on earlier research in the field, for creating a multi-layered optical skin phantom out of PDMS is presented in this report. All the steps of creating a phantom, including for example the choice of materials and calculation of tissue-like target optical properties, are shown and discussed to aid other research groups in the development of phantoms for their own specific purposes. Linear relations between the concentration of nigrosin and the absorption coefficient of the resulting phantom for 405 nm and 630 nm are presented to enable the tunability of absorption. The nigrosin concentrations necessary for all layers of both fair- and dark-skinned phantoms for 405 nm and 630 nm are estimated using these equations, though the 630 nm relation could not accurately estimate the necessary nigrosin concentrations for the 630 nm dermis and hypodermis layers due to their low target μ_a values. All layers except the 405 nm dark epidermis were successfully fabricated. Stacking the layers to create multi-layered phantoms however resulted in a significant increase in absorption due to the interface between the layers.

There is much potential for future research on this topic. The relation between nigrosin concentration and μ_a coefficient should be explored further, using a wider range of concentrations and at more wavelengths of light, potentially even looking into other absorbing agents that can produce stable phantoms with even larger μ_a values than nigrosin. The same should be done for the scattering agent TiO_2 and its effect on the μ'$_s$ coefficient. The effect on absorption from the interface between stacked phantom layers should also be more extensively investigated. The research field is furthermore in need of more data on the optical properties of dark skin, from both *in vivo* and *in vitro* samples, so that dark skin can be more reliably replicated in optical skin phantoms.

Bibliography

[1] Odinwell, https://odinwell.com/, accessed: 2025-06-27.

[2] P. Ramakrishnan *et al.*, "Cytotoxic responses to 405 nm light exposure in mammalian and bacterial cells: Involvement of reactive oxygen species," *Toxicology in Vitro*, vol. 33, pp. 54–62, 2016, https://doi.org/10.1016/j.tiv.2016.02.011.

[3] A. Cougnard-Gregoire *et al.*, "Blue Light Exposure: Ocular Hazards and Prevention—A Narrative Review," *Ophthalmology and Therapy*, p. 755–788, 2023, doi: 10.1007/s40123-023-00675-3.

[4] Etikprövningsmyndigheten, https://etikprovningsmyndigheten.se/, accessed: 2025-07-21.

[5] K. Setchfield *et al.*, "Effect of skin color on optical properties and the implications for medical optical technologies: a review," *Journal of Biomedical Optics*, vol. 29, 2024, doi.org/10.1117/1.JBO.29.1.010901.

[6] W. Yim *et al.*, "3D-Bioprinted Phantom with Human Skin Phototypes for Biomedical Optics," *Advanced Materials*, vol. 35, 2022, https://doi.org/10.1002/adma.202206385.

[7] I. M. Gidado *et al.*, "Review of advances in the measurement of skin hydration based on sensing of optical and electrical tissue properties," *Sensors*, vol. 22, 2022, https://doi.org/10.3390/s22197151.

[8] M. A. Cichoń and A. Elbe-Bürger, "Epidermal/Dermal Separation Techniques and Analysis of Cell Populations in Human Skin Sheets," *Journal of Investigative Dermatology*, vol. 143, pp. 11–17, 2023, https://doi.org/10.1016/j.jid.2022.10.012.

[9] K. Setchfield *et al.*, "Relevance and utility of the in-vivo and ex-vivo optical properties of the skin reported in the literature: a review," *Biomedical Optics Express*, vol. 14, pp. 3555–3583, 2023, https://doi.org/10.1364/BOE.493588.

[10] K. Mojsiewicz-Pieńkowska *et al.*, "Comparative study of the percutaneous permeation and bioaccumulation of a cyclic siloxane using frozen-thawed and nonfrozen ex vivo human skin," *Toxicology in Vitro*, vol. 82, 2022, https://doi.org/10.1016/j.tiv.2022.105379.

[11] T. Lister *et al.*, "Optical properties of human skin," *Journal of Biomedical Optics*, vol. 17, 2012, https://doi.org/10.1117/1.JBO.17.9.090901.

[12] A. Wurbs *et al.*, "A human ex vivo skin model breaking boundaries," *Scientific Reports*, vol. 14, 2024, https://doi.org/10.1038/s41598-024-75291-7.

[13] S. Eberlin *et al.*, "The ex vivo skin model as an alternative tool for the efficacy and safety evaluation of topical products," *Alternatives to Laboratory Animals*, vol. 48, 2020, https://doi.org/10.1177/0261192920914193.

[14] K. Szymczak *et al.*, "Photoactivated Gallium Porphyrin Reduces Staphylococcus aureus Colonization on the Skin and Suppresses Its Ability to Produce Enterotoxin C and TSST-1," vol. 20, p. 5108–5124, 2023, doi: 10.1021/acs.molpharmaceut.3c00399.

[15] B. W. Pogue and M. S. Patterson, "Review of tissue simulating phantoms for optical spectroscopy, imaging and dosimetry," *Journal of Biomedical Optics*, vol. 11, 2006, https://doi.org/10.1117/1.2335429.

[16] A. Kumar *et al.*, "Normal and diabetic foot sole skin mimicking tissue phantom fulfillment for spectroscopic-based DFU diagnostics perspective," *AIP Advances*, vol. 14, 2024, https://doi.org/10.1063/5.0206988.

[17] A. I. Chen *et al.*, "Multilayered tissue mimicking skin and vessel phantoms with tunable mechanical, optical, and acoustic properties," *The International Journal of Medical Physics Research and Practice*, vol. 43, pp. 3117–3131, 2016, https://doi.org/10.1118/1.4951729.

[18] G. J. Greening *et al.*, "Characterization of thin poly(dimethylsiloxane)-based tissue-simulating phantoms with tunable reduced scattering and absorption coefficients at visible and near-infrared wavelengths," *Journal of Biomedical Optics*, vol. 19, 2014, doi: 10.1117/1.JBO.19.11.115002.

[19] D. M. M. de Bruin *et al.*, "Optical phantoms of varying geometry based on thin building blocks with controlled optical properties"," *Journal of Biomedical Optics*, vol. 15, 2010, https://doi.org/10.1117/1.3369003.

[20] M. S. Wróbel *et al.*, "Multi-layered tissue head phantoms for noninvasive optical diagnostics," *Journal of Innovative Optical Health Sciences*, vol. 8, 2015, https://doi.org/10.1142/S1793545815410059.

[21] A. M. Goldfain *et al.*, "Polydimethylsiloxane tissue-mimicking phantoms with tunable optical properties," *Journal of Biomedical Optics*, vol. 27, 2021, doi.org/10.1117/1.JBO.27.7.074706.

[22] M. S. Wróbel *et al.*, "Use of optical skin phantoms for preclinical evaluation of laser efficiency for skin lesion therapy," *Journal of Biomedical Optics*, vol. 20, 2015, https://doi.org/10.1117/1.JBO.20.8.085003.

[23] M. Wróbel *et al.*, "Measurements of fundamental properties of homogeneous tissue phantoms," *Journal of Biomedical Optics*, vol. 20, 2015, https://doi.org/10.1117/1.JBO.20.4.045004.

[24] A. R. Young, "Chromophores in human skin," *Physics in Medicine Biology*, vol. 42, pp. 789–802, 1997, doi: 10.1088/0031-9155/42/5/004.

[25] K. Hoenes *et al.*, "405 nm and 450 nm Photoinactivation of Saccharomyces cerevisiae," *European Journal of Microbiology Immunology*, pp. 142–148, 2018, doi: 10.1556/1886.2018.00023.

[26] L. M. Jones *et al.*, "In Vitro Detection of Porphyrin-Producing Wound Bacteria with Real-Time Fluorescence Imaging," *Future Microbiology*, vol. 15, pp. 319–332, 2020, https://doi.org/10.2217/fmb-2019-0279.

[27] B. J. Tromberg *et al.*, "Properties of photon density waves in multiple-scattering media," *Applied Optics*, vol. 32, pp. 607–616, 1993, https://doi.org/10.1364/AO.32.000607.

[28] R. B. Saager *et al.*, "Multi-layer silicone phantoms for the evaluation of quantitative optical techniques in skin imaging," *Design and Performance Validation of Phantoms Used in Conjunction with Optical Measurement of Tissue II*, vol. 7567, 2010, https://doi.org/10.1117/12.842249.

[29] S. Prahl, "Everything I think you should know about Inverse Adding-Doubling," 2011, https://omlc.org/software/iad/manual.pdf.

[30] A. Afshari *et al.*, "Evaluation of the robustness of cerebral oximetry to variations in skin pigmentation using a tissue-simulating phantom," *Biomed Opt Express*, vol. 13, 2022, doi: 10.1364/BOE.454020.

[31] H. Jonasson *et al.*, "Absorption and reduced scattering coefficients in epidermis and dermis from a Swedish cohort study," *Journal of Biomedical Optics*, vol. 28, 2023, https://doi.org/10.1117/1.JBO.28.11.115001.

[32] M. Branchet *et al.*, "Skin Thickness Changes in Normal Aging Skin," *Gerontology*, vol. 36, pp. 28–35, 1990, https://doi.org/10.1159/000213172.

[33] K. Hwang *et al.*, "Thickness of skin and subcutaneous tissue of the free flap donor sites: A histologic study," *Microsurgery*, vol. 36, 2016, doi: 10.1002/micr.30000.

[34] F. Ayers *et al.*, "Fabrication and characterization of silicone-based tissue phantoms with tunable optical properties in the visible and near infrared domain," *Design and Performance Validation of Phantoms Used in Conjunction with Optical Measurements of Tissue*, vol. 6870, 2008, https://doi.org/10.1117/12.764969.

[35] Y. Shimojo *et al.*, "Measurement of absorption and reduced scattering coefficients in Asian human epidermis, dermis, and subcutaneous fat tissues in the 400- to 1100-nm wavelength range for optical penetration depth and energy deposition analysis," *Journal of Biomedical Optics*, vol. 25, 2020, doi.org/10.1117/1.JBO.25.4.045002.

[36] M. M. Houck and J. A. Siegel, *Fundamentals of Forensic Science (3rd ed)*, 2015.

[37] R. R. Triloki and B. Singh, "Absorbance and Transmittance measurement of CsI thin films," *DAE Symposium on Nuclear Physics*, vol. 58, 2013.

A

Appendices

A.1 Protocol for optical phantoms (one-sided mold)

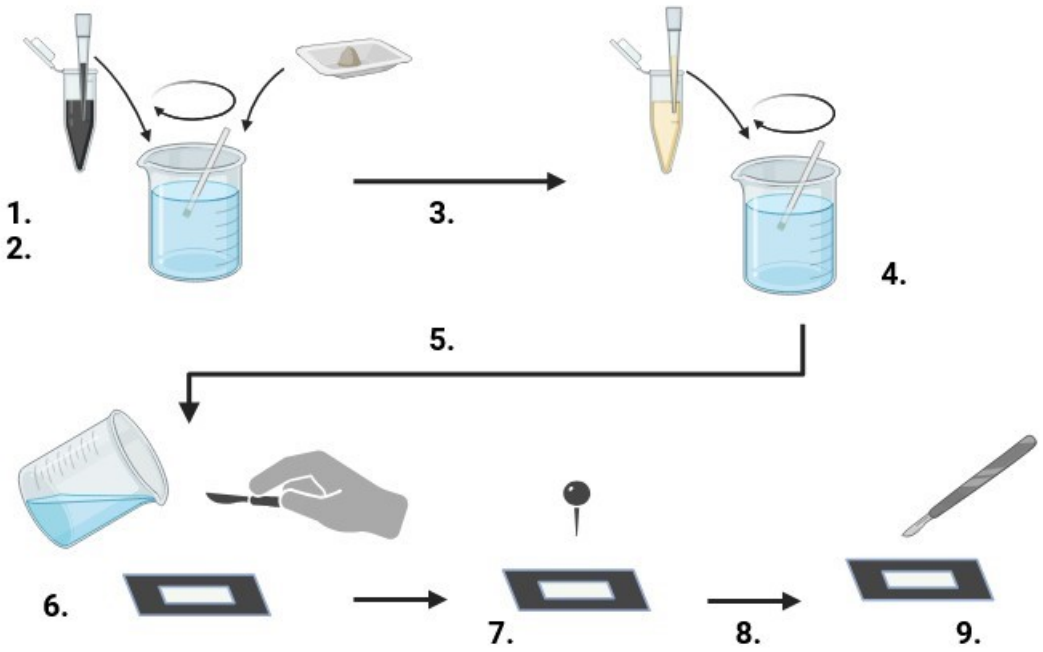

Figure A.1: Schematic protocol for creating PDMS optical phantoms using a one-sided mold. Made in Biorender.com.

1. Weigh the PDMS elastomer base into a lidded plastic cup.

2. Weigh the TiO_2 powder and add it to the PDMS base. Also pipette the 1% w/v nigrosin/ISO solution into the PDMS base. Stir by hand for 5-10 min, until the solution looks homogeneous.

3. Put the cup, with the lid closed, in an ultrasonic bath for 20 min. Stir the mixture by hand a few times to prevent the TiO_2 from settling.

4. Pipette the curing agent into the PDMS base solution and stir by hand for 10 min.

5. Put the cup, with the lid closed, into the ultrasonic bath for 15 min.

6. Fill a prepared mold by pouring in the silicone. Use a palette knife to even out the top in line with the edges of the mold.

7. Let the mold sit undisturbed on a flat surface for 10 minutes. Then use a sharp pin to pop any bubbles that might have risen to the surface.

8. Leave the molds on a level surface and let them cure, uncovered, for three days.

9. To remove the phantoms from the molds, run a razor blade along the walls of the mold to release the silicone from them. If using a thin mold made out of tape on a glass slide, remove the tape from the glass before pulling the silicone phantom from the glass, to help prevent the silicone from breaking.

A.2 Protocol for optical phantoms (double-sided mold)

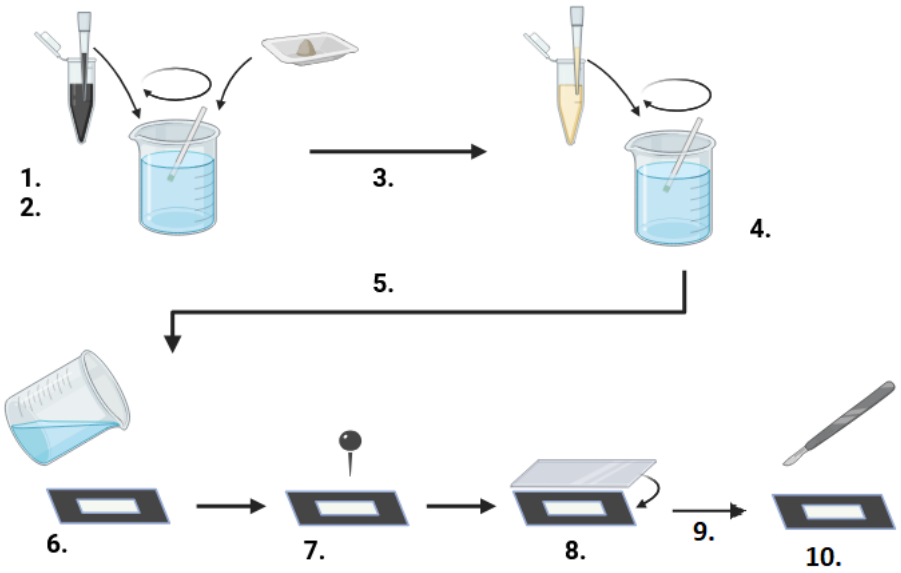

Figure A.2: Schematic protocol for creating PDMS optical phantoms using a double-sided mold. Made in Biorender.com.

1. Weigh the PDMS elastomer base into a lidded plastic cup.

2. Weigh the TiO_2 powder and add it to the PDMS base. Also pipette the 1% w/v nigrosin/ISO solution into the PDMS base. Stir by hand for 5-10 min, until the solution looks homogeneous.

3. Put the cup, with the lid closed, in an ultrasonic bath for 20 min. Stir the mixture by hand a few times to prevent the TiO_2 from settling.

4. Pipette the curing agent into the PDMS base solution and stir by hand for 10 min.

5. Put the cup, with the lid closed, into the ultrasonic bath for 15 min.

6. Fill a prepared mold by pouring in the silicone.

7. Let the mold sit undisturbed on a flat surface for 10 minutes. Then use a sharp pin to pop any bubbles that might have risen to the surface.

8. Add a glass plate on top of the mold by letting the glass plate first connect with a single side of the mold, and then tilting it until it is laying flat. Press down on the top glass plate to squeeze out the excess silicone. Tape around

the whole mold to keep the pressure stable during curing.

9. Leave the molds at a 45 degree angle and let them cure for three days.

10. To remove the phantoms from the molds, start by removing the tape. Then push a thin object under the top glass plate and separate it from the mold and the cured phantom inside. Use eye protection for this step. Lastly, run a razor blade along the walls of the mold to release the silicone from them. If using a thin mold made out of tape on a glass slide, remove the tape from the glass before pulling the silicone phantom from the glass, to help prevent the silicone from breaking

A.3 Calculation of target optical properties

The target optical properties for each phantom layer are based on previous research on the optical properties of human skin samples, but some calculations had to be made to get all of the values. The optical properties in fig. A.3 are taken directly from an article by Shimojo et al that measured the μ_a and μ'_s coefficients of *in vitro* skin samples from over 300 participants [35]. These data will be used as the starting point.

	Epidermis (Asian)*		Dermis*		Hypodermis*	
Wavelength	μ_a (cm^{-1})	μ'_s (cm^{-1})	μ_a (cm^{-1})	μ'_s (cm^{-1})	μ_a (cm^{-1})	μ'_s (cm^{-1})
405	33.2	99.5	4.3	64.6	6.2	25.6
632	9.4	55.5	0.7	30.6	0.7	17.2

Figure A.3: The average μ_a and μ'_s coefficients of *in vitro* skin samples from Asian participants [35].

All skin samples in the study by Shimojo et al were taken from Asian participants. In this thesis, I will assume that the dermis and hypodermis layers have the same optical properties for all FST phototypes. I will also assume that the Asian participants would fit in FST type III to IV.

To get reasonable target optical properties for the two epidermis phantom versions (FST I-II and FST V-VI, respectively), the values for the Asian epidermis in fig. A.3 have to be modified. According to a meta study by Setchfield et al that compiled the measured optical properties of *in vivo* samples of different skin colours over the wavelengths 400 nm to 1000 nm, fair skin (FST I-II) has on average 28% lower μ_a values and 27% lower μ'_s values than FST III-IV skin, while dark skin (FST V-VI) on average has 67% higher μ_a values and 7% lower μ'_s values than FST III-IV skin [5]. It should however be noted that the distribution of skin phototypes among the participants in the studies combined into the meta study by Setchfield et al was heavily skewed towards the lower (more fair-skinned) phototypes, and the FST V-VI data is based on only 12 individuals for the μ_a values and 7 individuals for the μ'_s values [5]. This means that there is a large uncertainty in the relation between the optical properties of FST III-IV and FST V-VI. Nevertheless, these average differences in the μ_a and μ'_s coefficients between phototypes were assumed to be caused solely by the optical properties of the epidermis, and the μ_a and μ'_s coefficients for the Asian epidermis was modified accordingly to create target optical properties for a fair and a dark epidermis, respectively. See fig. A.4 for the resulting values.

Wavelength	Epidermis (Asian)*		Epidermis (fair)**		Epidermis (dark)**	
	μ_a (cm^{-1})	μ'_s (mm^{-1})	μ_a (mm^{-1})	μ'_s (mm^{-1})	μ_a (mm^{-1})	μ'_s (mm^{-1})
405	33.2	99.5	23.9	72.6	55.4	92.5
632	9.4	55.5	6.8	40.5	15.7	51.6

Figure A.4: The μ_a and μ'_s coefficients of Asian epidermis, according to Shimojo et al [35], and estimated μ_a and μ'_s coefficients for fair (FST I-II) and dark (FST V-VI) epidermis, modified from the Asian epidermis data according to the relationship between the optical properties of different phototypes as determined by Setchfield et al [5].

Compiling the calculated results for the fair and the dark epidermis with the original data from Shimojo et al for the dermis and hypodermis layers into a single table, we get fig. A.5. This figure shows the target optical properties of every phantom layer for both 405 nm and 630 nm.

Wavelength	Epidermis (fair)**		Epidermis (dark)**		Dermis*		Hypodermis*	
	μ_a (cm^{-1})	μ'_s (cm^{-1})	μ_a (cm^{-1})	μ'_s (cm^{-1})	μ_a (cm^{-1})	μ'_s (cm^{-1})	μ_a (cm^{-1})	μ'_s (cm^{-1})
405	23.9	72.6	55.4	92.5	4.3	64.6	6.2	25.6
632	6.8	40.5	15.7	51.6	0.7	30.6	0.7	17.2

Figure A.5: The target optical properties of every phantom layer.

A.4 Example calculation of μ_a

This appendix presents an example calculation of how an absorbance value is converted to an absorption coefficient. This specific example is based on a 2.5 mm thick PDMS sample with 20 μl/g of 1% w/v nigrosin/ISO that is measured at a wavelength of 630 nm.

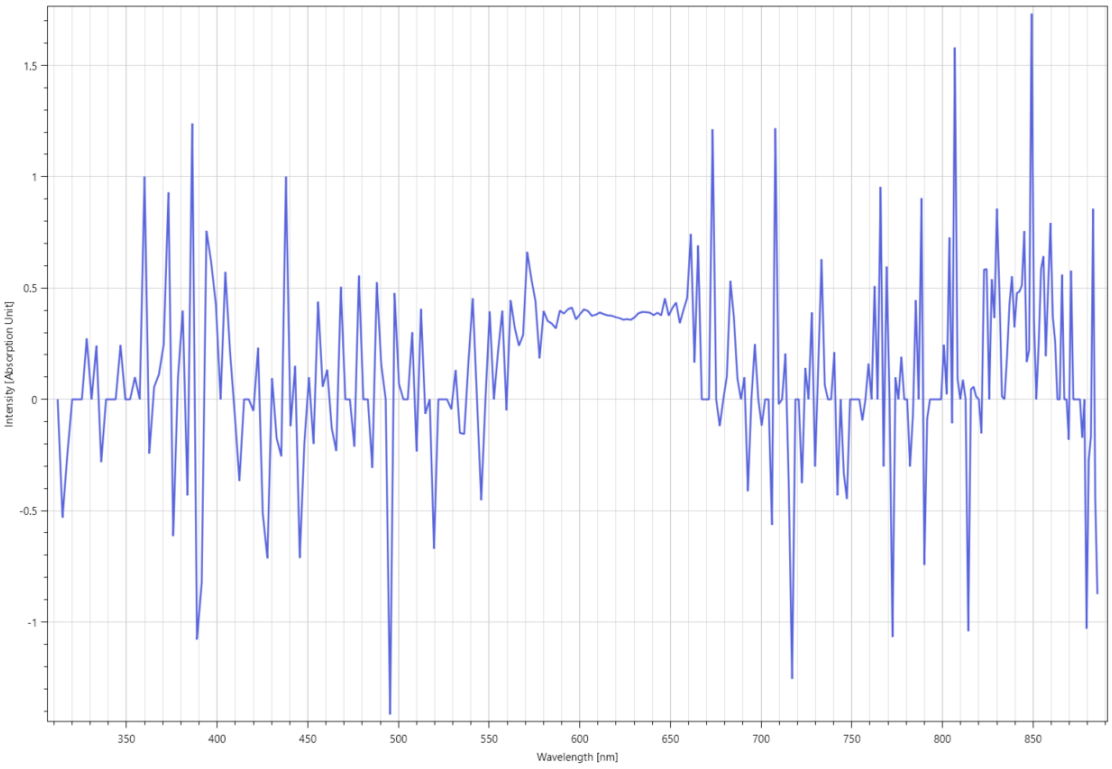

Figure A.6: Absorbance value at 630 nm for a 2.5 mm thick PDMS sample with 20 μl/g of 1% w/v nigrosin/ISO.

Fig. A.6 above shows the absorbance spectra for the PDMS sample. At exactly 630 nm, the absorbance was measured to 0.37.

Absorbance can be converted to absorption using this formula [37]:

$$A = 2.303(\alpha/t)$$

where A = absorption coefficient [cm^{-1}], α = absorbance, and t = sample thickness [cm]. Using the absorbance value from the specific example shown in the graph above, the function becomes:

$$A = 2.303(0.37/0.25cm) = 3.41cm^{-1}$$

This gives us that a concentration of 20 μl/g of 1% w/v nigrosin/ISO resulted in a PDMS sample with an absorption coefficient of 3.41 cm^{-1} at 630 nm.

DEPARTMENT OF SOME SUBJECT OR TECHNOLOGY
CHALMERS UNIVERSITY OF TECHNOLOGY
Gothenburg, Sweden
www.chalmers.se

CHALMERS
UNIVERSITY OF TECHNOLOGY